# Aggressive Maneuvering of a Quadrotor with a Cable-Suspended Payload

Sarah Tang

***Abstract*—This work examines the system of a quadrotor carrying a cable-suspended payload. As a motivating application, we demonstrate the "load-transport maneuver", where the quadrotor picks up an object with a cable mechanism, transports it through an environment, and drops it into a target location, mimicking the process of Christmas tree harvesting by human-piloted helicopters. We derive the coordinate-free dynamics for the system, which we model as a hybrid dynamical system, explore its differential flatness properties, and develop nonlinear controllers for its subsystems. We then present a trajectory generation technique that accounts for the switches of the hybrid system. Finally, we provide experimental validation on a quadrotor platform.**

## I. Introduction

The use of unmanned aerial vehicles (UAVs), in particular quadrotors, has recently become popular for a variety of tasks, including multi-agent path planning [33], mapping and exploration [27], and even acrobatic performances [2]. In addition, they have been applied to payload manipulation. For example, quadrotors have been successfully used for cooperative construction [18], grasping [32], and object transportation [26]. However, a payload held by a gripper can undesirably increase the inertia of the system.

An alternative is to attach the load to the quadrotor via a cable suspension, thereby retaining more of the vehicle's agility. Past related works for helicopters with slung-loads [3], [24] and quadrotors with cable-suspended loads [5], [6] have focused on stabilization of the load or minimization of load swing while traversing trajectories. In contrast, we hope to take advantage of the entire range of motion and consider trajectories with large load swings, load pick-ups and releases, and periods of zero cable tension where the load temporarily undergoes free-fall.

In particular, we are motivated by the process of Christmas tree harvesting [35], where a skilled pilot picks up trees and flings them into a truck-bed. We wish to mimic this process, which we will refer to as the "load-transport maneuver", with a quadrotor. To move loads quickly from their pick-up to their target locations, both the quadrotor and loads must experience large attitudes. In addition, pick-ups and releases of loads become transitions between two sets of dynamics.

Thus, we are motivated to view our system as a hybrid dynamical system. In one subsystem, which we will refer to as the "quadrotor-with-load subsystem", the quadrotor is actively controlling the load. In the other, the "quadrotor subsystem", the load has been released - the quadrotor motion is actively controlled while load is undergoing projectile motion.

Past work has developed a nonlinear controller for tracking of the load position, load attitude, and quadrotor attitude in the quadrotor-with-load subsystem [30], [29]. This controller has been proven to have almost global stability properties and experimentally verified on a quadrotor platform. The goal of this work is to extend this existing body of research by analyzing the complete hybrid system. To this end, we unify a number of techniques in geometric mechanics, differential flatness analysis, and control that were previously developed for various other non-hybrid systems. In addition, we propose a trajectory generation method that accounts for the switching dynamics of the hybrid system and produces continuous trajectories through these transitions. Finally, we demonstrate the execution of the load-transport maneuver on an Asctec Hummingbird [1] quadrotor, which unlike previous experiments, also includes switching between the two subsystems.

## II. Related Work

We use a number of geometric techniques to analyze the dynamics of our system. In particular, we use methods proposed by Lee [12] to develop Euler-Lagrange equations for mechanical systems that evolve on Lie groups. These methods have been successfully used to analyze the 3D pendulum [13], [16] and the spherical pendulum [14]. A global, geometric view of hybrid systems has also been introduced by [28], who propose definitions of traditional concepts in dynamical systems to hybrid systems, such as hybrifolds, hybrid flows, topological equivalence between hybrid systems, and $\omega$-limit points. However, this work is still in its early stages.

A number of techniques have been developed in planning and control for quadrotors. In trajectory generation, there are two main types of approaches. One of the most prominent probabilistic methods is Rapidly-Exploring Random Trees [11], and many variations have been proposed, included LQR trees [31] and RRT* [9]. These techniques randomly explore the space while taking into account system dynamics to generate feasible paths. Deterministic approaches attempt to find optimal trajectories. For example, Hehn et al. [8], [7] use Pontryagin's Minimum Principle to design minimum-time trajectories. Alternatively, Mellinger et al. [20], [19] note that the quadrotor is a differentially flat system [23] and plan in the lower-dimensional flat output space. They generate minimum snap trajectories by solving a constrained Quadratic Program (QP). Richter et al. [25] similarly generate optimal polynomial trajectories with a QP. However, they reformulate the problem as an unconstrained QP, which provides more numerical stability.

Early work in quadrotor control relied on linear PID or LQR controllers for a dynamic model linearized about the hover state [22]. However, the major drawback of these controllers is that they are only valid near the equilibrium hover configuration. Alternatively, nonlinear geometric controllers offer global or almost-global properties. Lee et al. [15] proposes such a controller for a quadrotor.

This type of geometric control has, in particular, been successful for controlling our system of interest, the quadrotor with a cable-suspended load. Sreenath et al. [30] propose a geometric controller for a planar model of the quadrotor-with-load subsystem and Sreenath et al. [29] adapts the controller for the full 3D model. This type of controller has also been used for cooperative manipulation of cable-suspended loads by quadrotor teams [17].

## III. Dynamic Model

We begin by modeling the dynamics of the system. We model the quadrotor and the load as a hybrid dynamical system: again, we will refer to the case where the cable-connection is taut as the "quadrotor-with-load" subsystem and the case where the load has detached from the cable as the "quadrotor" subsystem. The term system will, in general, refer to the complete hybrid dynamics while subsystem will refer to a specific set of dynamics. Fig. 1 illustrates the system and its two subsystems. We treat the quadrotor as a rigid-body and the load as a point-mass.

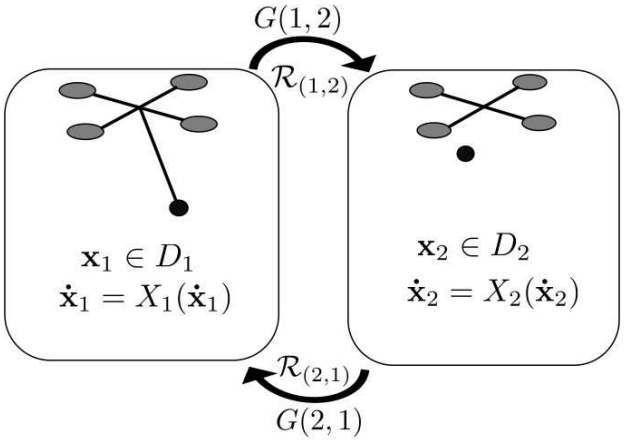


Fig. 1: Quadrotor with a cable-suspended load hybrid system

We describe a hybrid dynamical system with the 6-tuple:

$$H = (\mathcal{S}, E, \mathcal{D}, \mathcal{X}, \mathcal{G}, \mathcal{R}), \tag{1}$$

with variables defined in Table I.

### A. Quadrotor dynamics

We first derive the dynamics of the simpler quadrotor subsystem. Its configuration manifold is $\mathbb{R}^2 \times SE(3)$, with states:

$$\mathbf{x} = [\mathbf{x}_L \;\; \dot{\mathbf{x}}_L \;\; \mathbf{x}_Q \;\; \dot{\mathbf{x}}_Q \;\; {}^{\mathcal{I}}R_{\mathcal{B}} \;\; {}^{\mathcal{I}}\Omega_{\mathcal{B}}^{\mathcal{B}}]^T \tag{2}$$

For brevity, we drop subscripts and superscripts with the understanding that within Section III, $R = {}^{\mathcal{I}}R_{\mathcal{B}}$ and $\Omega = {}^{\mathcal{I}}\Omega_{\mathcal{B}}^{\mathcal{B}}$.

TABLE I: Variables of the quadrotor with load system

| | |
|---|---|
| $\mathcal{S} = \{1, ..., k\}$ | Subsystem indicies, $k \in \{\mathbb{Z} \mid k \geq 1\}$ |
| $E = \{(i,j) : i,j \in \mathcal{S}\}$ | Edges between subsystems, $E \subset \mathcal{S} \times \mathcal{S}$ |
| $\mathcal{D} = \{D_i : i \in \mathcal{S}\}$ | Domains of subsystems, $D_i \subset \mathbb{R}^n$ |
| $\mathcal{X} = \{X_i : i \in \mathcal{S}\}$ | Vector field describing $i$th subsystem |
| $\mathcal{G} = \{G(e) : e \in E\}$ | Guards between subsystems, $G(e) \subset D_i$ |
| $\mathcal{R} = \{R_e : e \in E\}$ | Resets between subsystems, $R_e : G(e) \to D_j$ |
| $\mathcal{I}$ | Inertial world frame, with axes $\mathbf{e}_i$ |
| $\mathcal{B}$ | Body frame of quad, with axes $\mathbf{b}_i$ |
| $g = 9.81 m/s^2$ | Gravity constant |
| $m_Q, m_L \in \mathbb{R}$ | Mass of quadrotor, load |
| $\mathbb{I}$ | Inertia tensor of quadrotor |
| $f \in \mathbb{R}$ | Magnitude of thrust on quadrotor |
| $\mathbf{M} \in \mathbb{R}^3$ | Moment vector on quadrotor, in $\mathcal{B}$ |
| $l \in \mathbb{R}$ | Length of suspension cable |
| $T \in \mathbb{R}$ | Magnitude of tension in cable |
| $\mathbf{x}_Q, \mathbf{x}_L \in \mathbb{R}^3$ | Position vector of quadrotor, load, in $\mathcal{I}$ |
| $\mathbf{p} \in \mathbb{S}^2$ | Unit vector from quadrotor to load, in $\mathcal{I}$ |
| $\omega \in \mathbb{R}^2$ | Angular velocity of load, in $\mathcal{I}$ |
| ${}^{\mathcal{I}}R_{\mathcal{B}} \in SO(3)$ | Rotation matrix of quadrotor from $\mathcal{B}$ to $\mathcal{I}$ |
| ${}^{\mathcal{I}}\Omega_{\mathcal{B}}^{\mathcal{B}} \in \mathbb{R}^3$ | Angular velocity of quadrotor, in $\mathcal{B}$ |

Fig. 2 illustrates the coordinate frames and external forces and moments on the quadrotor, where frame $\mathcal{C}$ is the intermediate frame after a yaw rotation. The load simply undergoes projectile motion and is omitted from the image.

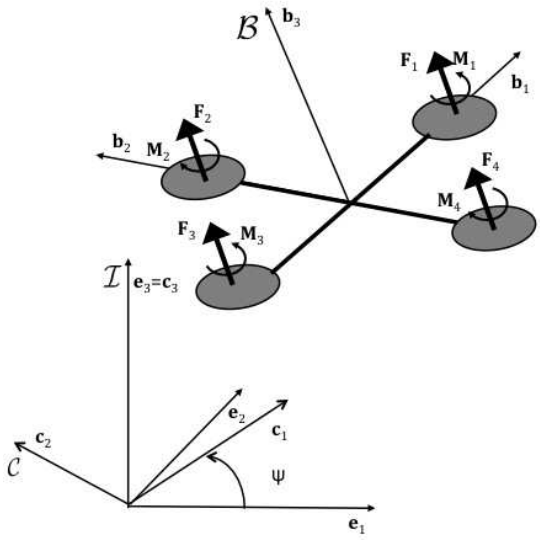


Fig. 2: Coordinate frames and external forces on the quadrotor

The quadrotor is propelled by four rotors, with the front and back rotors rotating in one direction and the left and right rotors rotating in the other. We can command each rotor $i$ to an angular speed $\omega_{r_i}$. The resulting magnitudes of force and moment are given as functions of angular speed as:

$$f_i = k_F \omega_{r_i}^2 \tag{3}$$

$$M_i = k_M \omega_{r_i}^2, \tag{4}$$

where the motor constants $k_F$ and $k_M$ can be found through calibration. These can then be related to the total external force

and moment on the quadrotor with:

$$\begin{bmatrix} f \\ \mathbf{M} \end{bmatrix} = \begin{bmatrix} k_F & k_F & k_F & k_F \\ 0 & k_F l_Q & 0 & -k_F l_Q \\ -k_F l_Q & 0 & k_F l_Q & 0 \\ k_M & -k_M & k_M & -k_M \end{bmatrix} \begin{bmatrix} \omega_{r_1}^2 \\ \omega_{r_2}^2 \\ \omega_{r_3}^2 \\ \omega_{r_4}^2 \end{bmatrix}, \quad (5)$$

where $l_Q$ is the distance from the motor to the center of mass, or the quadrotor arm length. $f$ acts orthogonal to the quadrotor body along the $\mathbf{b}_3$ axis, and $\mathbf{M}$ is a $3\times1$ moment vector acting about the body-frame axes. Given desired force and moments, Eq. 5 can be inverted to give the desired angular speeds of each motor. Thus, $f$ and $\mathbf{M}$ are treated as the quadrotor's control inputs.

The quadrotor's equations of motion can then be derived from the Newton-Euler equations:

$$\mathbf{F} = fR\mathbf{e}_3 - m_Q g\mathbf{e}_3 = m_Q\ddot{\mathbf{x}}_Q \quad (6)$$

$$\mathbf{M} = \Omega \times [\mathbb{I}]_{\mathcal{B}}\Omega + [\mathbb{I}]_{\mathcal{B}}\dot{\Omega} \quad (7)$$

Here, $[\mathbb{I}]_{\mathcal{B}}$ denotes the inertia tensor as a matrix in frame $\mathcal{B}$, and $\dot{\Omega}$ is the angular acceleration expressed in the body-frame.

The equations of motion for the entire subsystem are:

$$\frac{d}{dt}\mathbf{x}_L = \dot{\mathbf{x}}_L \quad (8)$$

$$\ddot{\mathbf{x}}_L = -g\mathbf{e}_3 \quad (9)$$

$$\frac{d}{dt}\mathbf{x}_Q = \dot{\mathbf{x}}_Q \quad (10)$$

$$\ddot{\mathbf{x}}_Q = \frac{f}{m_Q}R\mathbf{e}_3 - g\mathbf{e}_3 \quad (11)$$

$$\dot{R} = R\hat{\Omega} \quad (12)$$

$$\dot{\Omega} = [\mathbb{I}]_{\mathcal{B}}^{-1}\left(\mathbf{M} - \Omega \times [\mathbb{I}]_{\mathcal{B}}\Omega\right) \quad (13)$$

### *B. Quadrotor-with-load dynamics*

Next, we derive the equations of motion of the quadrotor-with-load subsystem. A traditional approach might first represent the rotation matrix with a local coordinate system. However, these coordinates, for example Euler angles, often contain points of singularity. In addition, they can be ambiguous; for example, there are 24 sets of Euler angles. These angles also result in equations of motion with complicated trigonometric functions. Similarly, traditional approaches would deal with the unit vector $\mathbf{p}$ on $\mathbb{S}^2$ by describing it with two angles or by carrying around the unit-length constraint. This again results in complex dynamical equations.

We wish to find a coordinate-free representation of the dynamics that gives the equations of motion in a compact, unambiguous, singularity-free manner. To this end, we employ the approach developed by Lee [12], [13], [14], [16] which uses Hamilton's principle to develop the Euler-Lagrange equations for mechanical systems that evolve on a Lie group.

To begin, recall the action integral, defined as:

$$S = \int_{t_1}^{t_2} \mathcal{L}\ dt$$

Here, $\mathcal{L} = \mathcal{T} - \mathcal{U}$ is the Lagrangian of the system and $\mathcal{T}, \mathcal{U}$ denote the kinetic and potential energy, respectively.

Hamilton's principle of least action states that the path a conservative mechanical system takes from configuration $\mathbf{q}_1$ at $t_1$ to $\mathbf{q}_2$ at $t_2$, where $\mathbf{q}$ is the set of generalized coordinates for the system, is the one for which the action integral is an extremum. This is often stated as:

$$\delta S = \int_{t_1}^{t_2} \delta\mathcal{L}\ dt = 0,$$

where $\delta\mathcal{L}$ is the variation of the Lagrangian. For systems with applied non-conservative forces and moments, the extended Hamilton's principle applies:

$$\delta S = \int_{t_1}^{t_2} (\delta W + \delta\mathcal{L})\ dt = 0 \quad (14)$$

We apply Eq. 14 to the quadrotor-with-load subsystem. The configuration manifold of this subsystem is $\mathbb{R}^2 \times \mathbb{S}^2 \times SO(3)$, with states:

$$\mathbf{x} = \begin{bmatrix} \mathbf{x}_L & \dot{\mathbf{x}}_L & \mathbf{p} & \omega & R & \Omega \end{bmatrix}^T \quad (15)$$

We begin by calculating the Lagrangian. The total kinetic energy is comprised of the translational kinetic energy of the quadrotor and load and the rotational kinetic energy of the quadrotor:

$$\mathcal{T} = \frac{1}{2}m_Q\dot{\mathbf{x}}_Q \cdot \dot{\mathbf{x}}_Q + \frac{1}{2}m_L\dot{\mathbf{x}}_L \cdot \dot{\mathbf{x}}_L + \frac{1}{2}\Omega \cdot \mathbb{I} \cdot \Omega \quad (16)$$

The quadrotor and load states are related by the constraints:

$$\mathbf{x}_Q = \mathbf{x}_L - l\mathbf{p} \quad (17)$$

$$\dot{\mathbf{x}}_Q = \dot{\mathbf{x}}_L - l\dot{\mathbf{p}} \quad (18)$$

This allows us to express Eq. 16 in terms of subsystem states:

$$\begin{aligned} \mathcal{T} &= \frac{1}{2}m_Q(\dot{\mathbf{x}}_L - l\dot{\mathbf{p}}) \cdot (\dot{\mathbf{x}}_L - l\dot{\mathbf{p}}) + \frac{1}{2}m_L\dot{\mathbf{x}}_L \cdot \dot{\mathbf{x}}_L + \frac{1}{2}\Omega \cdot \mathbb{I} \cdot \Omega \\ &= \frac{1}{2}(m_Q + m_L)\dot{\mathbf{x}}_L \cdot \dot{\mathbf{x}}_L - m_Q l\dot{\mathbf{x}}_L \cdot \dot{\mathbf{p}} \\ &\qquad + \frac{1}{2}m_Q l^2\dot{\mathbf{p}} \cdot \dot{\mathbf{p}} + \frac{1}{2}\Omega \cdot \mathbb{I} \cdot \Omega \end{aligned} \quad (19)$$

The potential energy $\mathcal{U}$ only contains gravitational potential energy terms, and we again use the constraint Eq. 17:

$$\begin{aligned} \mathcal{U} &= m_Q g\mathbf{x}_Q \cdot \mathbf{e}_3 + m_L g\mathbf{x}_L \cdot \mathbf{e}_3 \\ &= m_L g(\mathbf{x}_L - l\mathbf{p}) \cdot \mathbf{e}_3 + m_L g\mathbf{x}_L \cdot \mathbf{e}_3 \\ &= (m_Q + m_L)g\mathbf{x}_L \cdot \mathbf{e}_3 - m_Q gl\mathbf{p} \cdot \mathbf{e}_3 \end{aligned} \quad (20)$$

We approximate the variation in kinetic energy using the first-order Taylor approximation:

$$\begin{aligned} \delta\mathcal{T} &= \mathcal{T}(\dot{\mathbf{x}}_L + \delta\dot{\mathbf{x}}_L, \dot{\mathbf{p}} + \delta\dot{\mathbf{p}}, \Omega + \delta\Omega) - \mathcal{T}(\dot{\mathbf{x}}_L, \dot{\mathbf{p}}, \Omega) \\ &\approx \frac{\partial\mathcal{T}}{\partial\dot{\mathbf{x}}_L}\delta\dot{\mathbf{x}}_L + \frac{\partial\mathcal{T}}{\partial\dot{\mathbf{p}}}\delta\dot{\mathbf{p}} + \frac{\partial\mathcal{T}}{\partial\Omega}\delta\Omega \\ &= ((m_Q + m_L)\dot{\mathbf{x}}_L - m_Q l\dot{\mathbf{p}}) \cdot \delta\dot{\mathbf{x}}_L \\ &\qquad + (-m_Q l\dot{\mathbf{x}}_L + m_Q l^2\dot{\mathbf{p}}) \cdot \delta\dot{\mathbf{p}} + [\mathbb{I}]_{\mathcal{B}}\Omega \cdot \delta\Omega \end{aligned} \quad (21)$$

Note that we have used the fact that the inertia matrix is symmetric and $\frac{1}{2}([\mathbb{I}]_{\mathcal{B}} + [\mathbb{I}]_{\mathcal{B}}^T) = [\mathbb{I}]_{\mathcal{B}}$. Similarly, for the

potential energy term:

$$\begin{aligned}\delta\mathcal{U} &= \mathcal{U}(\mathbf{x}_L + \delta\mathbf{x}_L, \mathbf{p} + \delta\mathbf{p}) - \mathcal{U}(\mathbf{x}_L, \mathbf{p}) \\ &\approx \frac{\partial \mathcal{U}}{\partial \mathbf{x}_L}\delta\mathbf{x}_L + \frac{\partial \mathcal{U}}{\partial \mathbf{p}}\delta\mathbf{p} \\ &= (m_Q + m_L)g\mathbf{e}_3 \cdot \delta\mathbf{x}_L - m_Q g l \mathbf{e}_3 \cdot \delta\mathbf{p} \end{aligned} \tag{22}$$

Next, we find the terms of the virtual work $\delta W$. Recall that for a system with $N$ applied forces $\mathbf{F}_i$ applied at positions $\mathbf{r}_i$, $M$ rigid bodies with applied moments $\mathbf{M}_i$, and $n$ generalized coordinates, the virtual work is:

$$\delta W = \sum_{i=1}^{N} \mathbf{F}_i \cdot \sum_{j=1}^{n} \frac{\partial \mathbf{r}_i}{\partial q_j}\delta q_j + \sum_{i=1}^{M} \mathbf{M}_i \cdot \sum_{j=1}^{n} \frac{\partial^{\mathcal{I}}\Omega^{\mathcal{B}_i}}{\partial \dot{q}_j}\delta q_j$$

For this subsystem, $q_j = \mathbf{x}_L, \mathbf{p}, R$. The only applied force is the thrust force $f$, acting at the quadrotor's center of mass, with associated virtual work:

$$\begin{aligned}\delta W_1 &= fR\mathbf{e}_3 \cdot \sum_{j=1}^{3} \frac{\partial \mathbf{x_Q}}{\partial q_j}\delta q_j \\ &= fR\mathbf{e}_3 \cdot \sum_{j=1}^{3} \frac{\partial (\mathbf{x}_L - l\mathbf{p})}{\partial q_j}\delta q_j \\ &= fR\mathbf{e}_3 \cdot (\delta\mathbf{x}_L - l\delta\mathbf{p}) \end{aligned} \tag{23}$$

The quadrotor is the only rigid body in the subsystem and is acted on by moment $\mathbf{M}$, with associated virtual work:

$$\begin{aligned}\delta W_2 &= \mathbf{M} \cdot \sum_{j=1}^{n} \frac{\partial \Omega}{\partial \dot{q}_j}\delta q_j \\ &= \mathbf{M} \cdot \frac{\partial (R^T\dot{R})^\vee}{\partial \dot{R}}\delta R \\ &= \mathbf{M} \cdot (R^T\delta R) \end{aligned} \tag{24}$$

Note that we do not consider the tension force, as it is a constraint force that contributes no virtual work.

Eqs. 21 - 24 allow us to rearrange Eq. 14 as variations in each generalized coordinate:

$$\begin{aligned}\delta S &= \int_{t_1}^{t_2} (\delta W_1 + \delta W_2 + \delta\mathcal{T} - \delta\mathcal{U})dt \\ &= \int_{t_1}^{t_2} \big( fR\mathbf{e}_3 \cdot (\delta\mathbf{x}_L - l\delta\mathbf{p}) + M \cdot (R^T\delta R) \\ &\qquad + ((m_Q + m_L)\dot{\mathbf{x}}_L - m_Q l\dot{\mathbf{p}}) \cdot \delta\dot{\mathbf{x}}_L \\ &\qquad + (-m_Q l\dot{\mathbf{x}}_L + m_Q l^2\dot{\mathbf{p}}) \cdot \delta\dot{\mathbf{p}} + \Omega^T[\mathbb{I}]_{\mathcal{B}} \cdot \delta\Omega \\ &\qquad -(m_Q + m_L)g\mathbf{e}_3 \cdot \delta\mathbf{x}_L + m_Q g l \mathbf{e}_3 \cdot \delta\mathbf{p}) \, dt \\ &= \int_{t_1}^{t_2} (((m_Q + m_L)\dot{\mathbf{x}}_L - m_Q l\dot{\mathbf{p}}) \cdot \delta\dot{\mathbf{x}}_L \\ &\qquad +(fR\mathbf{e}_3 - (m_Q + m_L)g\mathbf{e}_3) \cdot \delta\mathbf{x}_L) \, dt \\ &\quad + \int_{t_1}^{t_2} \big((m_Q l^2\dot{\mathbf{p}} - m_Q l\dot{\mathbf{x}}_L) \cdot \delta\dot{\mathbf{p}} \\ &\qquad +(m_Q g l\mathbf{e}_3 - flR\mathbf{e}_3) \cdot \delta\mathbf{p}) \, dt \\ &\quad + \int_{t_1}^{t_2} \big(\Omega^T[\mathbb{I}]_{\mathcal{B}} \cdot \delta\Omega + M \cdot (R^T\delta R)\big) \, dt \end{aligned} \tag{25}$$

While $\mathbf{x}_L$ and $\dot{\mathbf{x}}_L$ vary in $\mathbb{R}^3$, we must take care to properly define the infinitesimal variations $\delta R$ and $\delta\mathbf{p}$, as they vary on specific configuration manifolds.

From Bullo and Lewis [4], for a manifold $Q$ and point $x \in Q$, a curve in time at $x$ is defined as $\gamma(t) : I \to Q$, where:

- $I$ is some interval containing 0
- $\gamma(0) = x$

A variation of $\gamma(t)$ is a map $\gamma^\epsilon(t) : J \times I \to Q$ where:

- $I = [a, b]$, $J$ both contain 0
- $\gamma^0(t) = \gamma(t)\ \forall t \in I$
- $\gamma^\epsilon(a) = \gamma(a)\ \forall \epsilon \in J$
- $\gamma^\epsilon(b) = \gamma(b)\ \forall \epsilon \in J$

The corresponding infinitesimal variation is found with:

$$\delta\gamma(t) = \left.\frac{d}{d\epsilon}\right|_{\epsilon=0} \gamma^\epsilon(t) \in T_{\gamma(t)}Q \tag{26}$$

Lee [12] show that variations for curves $g(t)$ in a Lie group $G$ can be expressed using the exponential map:

$$g^\epsilon(t) = g(t)e^{\epsilon\eta(t)},$$

where $\eta(t) \in \mathfrak{g}$ and $\mathfrak{g}$ is the Lie algebra of $G$.

In our case, $R$ is defined on the Lie group $SO(3) = \{R : \mathbb{R}^3 \to \mathbb{R}^3 | R^TR = I, \det R = 1\}$, whose corresponding Lie algebra is the set of skew-symmetric matrices $\mathfrak{so}(3)$. Thus, we can represent a variation of an element $R \in SO(3)$ with exponential coordinates:

$$R^\epsilon = Re^{\epsilon\hat{\eta}},$$

where $\eta \in \mathbb{R}^3$. We find the infinitesimal variation with Eq. 26:

$$\delta R = \frac{d}{d\epsilon}\,|_{\epsilon=0} Re^{\epsilon\hat{\eta}} = R\hat{\eta}$$

This variation is derived by Lee et al. [13].

$\mathbf{p}$ is defined on the two-sphere $\mathbb{S}^2 = \{\mathbf{p} \in \mathbb{R}^3 | \mathbf{p} \cdot \mathbf{p} = 1\}$. $\mathbb{S}^2$ is not itself a Lie group. However, the Lie group $SO(3)$ acts on $\mathbb{S}^2$ transitively; that is, for $\forall q_1, q_2 \in \mathbb{S}^2, \exists R$ such that $q_2 = Rq_1$. Thus, we can use the variation of $R$ to write the variation of $\mathbf{p}$:

$$\mathbf{p}^\epsilon = e^{\epsilon\hat{\xi}}\mathbf{p},$$

where $\xi \in \mathbb{R}^3$. The corresponding infinitesimal variation is:

$$\delta\mathbf{p} = \frac{d}{d\epsilon}\,|_{\epsilon=0} e^{\epsilon\hat{\xi}}\mathbf{p} = \hat{\xi}\mathbf{p}$$

These variations on $\mathbb{S}^2$ are described by Lee et al. [16].

Thus, we can define variations:

$$\delta\mathbf{p} = \xi \times \mathbf{p} \in T_{\mathbf{p}}\mathbb{S}^2, \text{ where } \xi \in \mathbb{R}^3,\ \xi \cdot \mathbf{p} = 0 \tag{27}$$

$$\delta R = R\hat{\eta} \in T_R SO(3), \text{ where } \eta \in \mathbb{R}^3,\ \hat{\eta} \in \mathfrak{so}(3) \tag{28}$$

Differentiation of Eqs. 27 and 28 gives the variations:

$$\begin{aligned}\delta\dot{\mathbf{p}} &= \dot{\xi}\times\mathbf{p} + \xi\times\dot{\mathbf{p}} \quad (29)\\ \delta\dot{R} &= \dot{R}\hat{\eta} + R\hat{\dot{\eta}}\\ \delta\hat{\Omega} &= \delta(R^T\dot{R})\\ &= \delta R^T\dot{R} + R^T\delta\dot{R}\\ &= (R\hat{\eta})^T\dot{R} + R^T(\dot{R}\hat{\eta} + R\hat{\dot{\eta}})\\ &= \hat{\eta}^T\hat{\Omega} + \hat{\Omega}\hat{\eta} + \hat{\dot{\eta}}\\ &= \widehat{\hat{\Omega}\eta} + \hat{\dot{\eta}}\\ \delta\Omega &= \hat{\Omega}\eta + \dot{\eta} \quad (30)\end{aligned}$$

With Eqs. 27 - 30, we can write each integral in Eq. 25 in terms of $\delta\mathbf{x}_L$, $\xi$ and $\eta$, all of which are variations in $\mathbb{R}^3$. We evaluate each integral through integration by parts, as is traditionally done when deriving the Euler-Lagrange equations from Hamilton's principle. The details of the integration can be found in Appendix A.

In particular, we note that geometrically, the tangent space at point $\mathbf{p}$ is a plane tangent to the sphere at $\mathbf{p}$. Thus, a point $\mathbf{p}$ and its time derivative satisfy:

$$\mathbf{p}\cdot\dot{\mathbf{p}} = 0 \quad (31)$$

This can be written in terms of angular velocity as:

$$\dot{\mathbf{p}} = \omega\times\mathbf{p}, \quad (32)$$

where $\{\omega\in\mathbb{R}^3|\mathbf{p}\cdot\omega = 0\}$. We can then see that:

$$\mathbf{p}\cdot\dot{\omega} = 0 \quad (33)$$

Eqs. 31 - 33 are used when appropriate. The result is:

$$\begin{aligned}\delta S = \int_{t_1}^{t_2} &((m_Q l\ddot{\mathbf{p}} - (m_Q+m_L)\ddot{\mathbf{x}}_L\\ &\quad + fR\mathbf{e}_3 - (m_Q+m_L)g\mathbf{e}_3)\cdot\delta\mathbf{x}_L)\,dt\\ + \int_{t_1}^{t_2} &((\mathbf{p}\times(m_Q g l\mathbf{e}_3 - flR\mathbf{e}_3\\ &\quad + m_Q l\ddot{\mathbf{x}}_L - m_Q l^2\ddot{\mathbf{p}}))\cdot\xi)\,dt\\ + \int_{t_1}^{t_2} &\Big((-\Omega\times[\mathbb{I}]_{\mathcal{B}}\Omega - [\mathbb{I}]_{\mathcal{B}}\dot{\Omega} + M)\cdot\eta\Big)\,dt = 0\end{aligned} \quad (34)$$

Setting each variation to 0, Eq. 34 yields:

$$m_Q l\ddot{\mathbf{p}} - (m_Q+m_L)\ddot{\mathbf{x}}_L - (m_Q+m_L)g\mathbf{e}_3 + fR\mathbf{e}_3 = 0 \quad (35)$$

$$\mathbf{p}\times(m_Q g\mathbf{e}_3 - fR\mathbf{e}_3 + m_Q\ddot{\mathbf{x}}_L - m_Q l\ddot{\mathbf{p}}) = 0 \quad (36)$$

$$-\Omega\times[\mathbb{I}]_{\mathcal{B}}\Omega - [\mathbb{I}]_{\mathcal{B}}\dot{\Omega} + M = 0 \quad (37)$$

With details in Appendix A, Eqs. 35 - 37 simplify to:

$$\frac{d}{dt}\mathbf{x}_L = \dot{\mathbf{x}}_L \quad (38)$$

$$(m_Q+m_L)(\ddot{\mathbf{x}}_L + g\mathbf{e}_3) = (\mathbf{p}\cdot fR\mathbf{e}_3 - m_Q l(\dot{\mathbf{p}}\cdot\dot{\mathbf{p}}))\mathbf{p} \quad (39)$$

$$\dot{\mathbf{p}} = \omega\times\mathbf{p} \quad (40)$$

$$m_Q l\dot{\omega} = -\mathbf{p}\times fR\mathbf{e}_3 \quad (41)$$

$$\dot{R} = R\hat{\Omega} \quad (42)$$

$$[\mathbb{I}]_{\mathcal{B}}\dot{\Omega} = \mathbf{M} - \Omega\times[\mathbb{I}]_{\mathcal{B}}\Omega \quad (43)$$

### C. Full hybrid system model

We are now ready to formally define the full hybrid dynamical system. Recall Eq. 1:

$$H = (\mathcal{S}, E, \mathcal{D}, \mathcal{X}, \mathcal{G}, \mathcal{R})$$

For this system, $k = 2$, $\mathcal{S} = \{1, 2\}$, and $E = \{(1, 2), (2, 1)\}$. Let 1 denote the quadrotor-with-load subsystem and 2 denote the quadrotor subsystem. Recall:

$$\begin{aligned}\mathbf{x}_1 &= [\mathbf{x}_L \;\; \dot{\mathbf{x}}_L \;\; \mathbf{p} \;\; \omega \;\; R \;\; \Omega]^T\\ \mathbf{x}_2 &= [\mathbf{x}_L \;\; \dot{\mathbf{x}}_L \;\; \mathbf{x}_Q \;\; \dot{\mathbf{x}}_Q \;\; R \;\; \Omega]^T\end{aligned}$$

The transition from subsystem 1 to 2 occurs when the load reaches a desired release position, denoted $\mathbf{x}_r$, and release velocity, denoted $\dot{\mathbf{x}}_r$. The transition back occurs when the quadrotor and the load are exactly a cable-length apart and the end of the cable is in position to pick up the load. This defines the guards:

$$\begin{aligned}\mathcal{G} = \{&G(1,2) = \{\mathbf{x}_1|\mathbf{x}_L = \mathbf{x}_r, \dot{\mathbf{x}}_L = \dot{\mathbf{x}}_r\},\\ &G(2,1) = \{\mathbf{x}_2|\|\mathbf{x}_Q - \mathbf{x}_L\| = l\}\}\end{aligned} \quad (44)$$

In terms of the resets, when the quadrotor releases the load, all states remain the same. The reset from subsystem 1 to subsystem 2 is thus an identity map incorporating the constraint equations Eqs. 17 - 18. When the quadrotor picks up the load, their positions remain the same across the switch. We model the pick-up as a nonelastic collision between the quadrotor and the load. Using the approximation $m_Q >> m_L$, the load assumes the velocity of the quadrotor. The quadrotor attitude states remain the same. This defines the resets:

$$\begin{aligned}\mathcal{R} = \{&R_{(1,2)} = [\mathbf{x}_L \;\; \dot{\mathbf{x}}_L \;\; \mathbf{x}_L - l\mathbf{p} \;\; \dot{\mathbf{x}}_L - l\dot{\mathbf{p}} \;\; R \;\; \Omega]^T,\\ &R_{(2,1)} = [\mathbf{x}_L \;\; \dot{\mathbf{x}}_L \;\; \frac{\mathbf{x}_Q - \mathbf{x}_L}{l} \;\; 0 \;\; R \;\; \Omega]^T\}\end{aligned} \quad (45)$$

## IV. Differential Flatness

A differentially flat system [23] is a system that has a set of flat outputs, where the states and inputs of the system can be derived as smooth functions of these flat outputs and their higher derivatives. Thus, rather than planning trajectories for the full state vector, which is usually high dimensional and has dynamically coupled variables, we can plan in the flat output space. This allows for planning in a lower-dimensional space where all variables are independent. Any smooth trajectory for the flat outputs can then be mapped back into feasible trajectories for the full set of states and inputs of the system.

We wish to define a similar notion for hybrid systems, which additionally includes switches between subsystems. A differentially flat hybrid system [29] is a system where:

1) Each subsystem is differentially flat.
2) All guards are functions of the flat outputs of their corresponding subsystem and their higher derivatives.
3) All resets have sufficiently smooth transition maps between the flat outputs of the two subsystems.

We propose that a quadrotor with a cable-suspended load is a differentially flat hybrid system, with the $\mathbf{y}_1 = [\mathbf{x}_L \;\; \psi]^T$ as flat outputs for the quadrotor-with-load subsystem and $\mathbf{y}_2 =$

$[\mathbf{x}_Q \ \ \psi]^T$ as the set of flat outputs for the quadrotor subsystem, where $\psi$ is the yaw angle of the quadrotor.

We can quickly see that the proposed flat outputs satisfy the requirements on the guards and resets. The $G(1,2)$ functions, $\mathbf{x}_L = \mathbf{x}_r$ and $\dot{\mathbf{x}}_L = \dot{\mathbf{x}}_r$, are clearly functions of the proposed flat output $\mathbf{x}_L$. The $G(2,1)$ function, $\|\mathbf{x}_Q - \mathbf{x}_L\| = l$, requires knowledge of $\mathbf{x}_L$. Recall that in the quadrotor subsystem, the load undergoes projectile motion. Thus, $\mathbf{x}_L$ is completely known from the initial state of the load in the subsystem. Thus, the $G(2,1)$ function is a function of only the flat output, $\mathbf{x}_Q$.

In the subsystem 1 to subsystem 2 reset, we derive the quadrotor position from $\mathbf{x}_Q = \mathbf{x}_L - l\mathbf{p}$. The vector $\mathbf{p}$ can be derived from the Newton's equation for the load:

$$\sum \mathbf{F}_L = -T\mathbf{p} - m_L g\mathbf{e}_3 = m_L \ddot{\mathbf{x}}_L \tag{46}$$

$$\mathbf{p} = \frac{T\mathbf{p}}{\|T\mathbf{p}\|} = \frac{-(\ddot{\mathbf{x}}_L + g\mathbf{e}_3)}{\|\ddot{\mathbf{x}}_L + g\mathbf{e}_3\|} \tag{47}$$

We see that $\mathbf{p}$ is a function of the flat output $\mathbf{x}_L$. The yaw angles are mapped with the identity map. In the transition from subsystem 2 to subsystem 1, the state $\mathbf{x}_L$ is known completely from its initial state within the subsystem and the yaw angles are again equal.

Finally, we prove that the proposed outputs are in fact flat outputs for their respective subsystems.

### A. Differential flatness of the quadrotor subsystem

We propose that $\mathbf{y}_2 = [\mathbf{x}_Q \ \ \psi]^T$ is the set of flat outputs for the quadrotor system, with state:

$$\mathbf{x}_2 = [\mathbf{x}_L \ \ \dot{\mathbf{x}}_L \ \ \mathbf{x}_Q \ \ \dot{\mathbf{x}}_Q \ \ {}^{\mathcal{I}}R_{\mathcal{B}} \ \ {}^{\mathcal{I}}\Omega_{\mathcal{B}}^{\mathcal{B}}]^T$$

and input:

$$\mathbf{u} = [f \ \ \mathbf{M}]^T$$

The load states are automatically known, as the load is simply undergoing projectile motion, and we only need to derive the quadrotor's states. This procedure is outlined by Mellinger and Kumar [19] and is repeated here, as the results will also be used for the quadrotor-with-load subsystem.

As illustrated in Fig. 2, let $\mathcal{I}$ be the inertial world frame, $\mathcal{C}$ be an intermediate frame after yaw rotation $\psi$, and $\mathcal{B}$ be a body-frame for the quadrotor. $\dot{\mathbf{x}}_Q$ and $\ddot{\mathbf{x}}_Q$, are known from simple differentiation of the quadrotor position. From the equation of motion Eq. 6:

$$f\mathbf{b}_3 = m_Q(\ddot{\mathbf{x}}_Q + g\mathbf{e}_3),$$

we can obtain the thrust and $\mathbf{b}_3$ body-frame vector with:

$$f = m_Q\|\ddot{\mathbf{x}}_Q + g\mathbf{e}_3\| \tag{48}$$

$$\mathbf{b}_3 = \frac{\ddot{\mathbf{x}}_Q + g\mathbf{e}_3}{\|\ddot{\mathbf{x}}_Q + g\mathbf{e}_3\|} \tag{49}$$

To find the rotation matrix, ${}^{\mathcal{I}}R_{\mathcal{B}}$, we use $\psi$ to define:

$$\mathbf{c}_1 = \begin{bmatrix}\cos(\psi) & \sin(\psi) & 0\end{bmatrix}^T \tag{50}$$

$$\mathbf{c}_2 = \begin{bmatrix}-\sin(\psi) & \cos(\psi) & 0\end{bmatrix}^T \tag{51}$$

Assuming a Z-Y-X rotation, the $\mathbf{c}_2 - \mathbf{b}_3$ plane is the same as the $\mathbf{b}_2 - \mathbf{b}_3$ plane. Thus, we can find the remaining two body-frame vectors:

$$\mathbf{b}_1 = \frac{\mathbf{c}_2 \times \mathbf{b}_3}{\|\mathbf{c}_2 \times \mathbf{b}_3\|} \tag{52}$$

$$\mathbf{b}_2 = \mathbf{b}_3 \times \mathbf{b}_1 \tag{53}$$

Assuming $\mathbf{b}_3$ is not parallel to $\mathbf{c}_1$, we can now define:

$$R = \begin{bmatrix}\mathbf{b}_1 & \mathbf{b}_2 & \mathbf{b}_3\end{bmatrix} \tag{54}$$

Next, we differentiate the equation of motion Eq. 6:

$$m_Q\dddot{\mathbf{x}}_Q = \dot{f}\mathbf{b}_3 + f\left({}^{\mathcal{I}}\Omega^{\mathcal{B}} \times \mathbf{b}_3\right) \tag{55}$$

Taking the $\mathbf{b}_3$ component:

$$\dot{f} = m_Q(\dddot{\mathbf{x}}_Q \cdot \mathbf{b}_3) \tag{56}$$

We can substitute this $\dot{f}$ back into Eq. 55:

$${}^{\mathcal{I}}\Omega^{\mathcal{B}} \times \mathbf{b}_3 = \frac{m_Q}{f}\dddot{\mathbf{x}}_Q - \frac{\dot{f}}{f}\mathbf{b}_3$$

Taking the $\mathbf{b}_1$ and $\mathbf{b}_2$ components, we find:

$$({}^{\mathcal{I}}\Omega^{\mathcal{B}} \times \mathbf{b}_3) \cdot \mathbf{b}_1 = \left(\frac{m_Q}{f}\dddot{\mathbf{x}}_Q - \frac{\dot{f}}{f}\mathbf{b}_3\right) \cdot \mathbf{b}_1 = {}^{\mathcal{I}}\Omega^{\mathcal{B}} \cdot \mathbf{b}_2 \tag{57}$$

$$({}^{\mathcal{I}}\Omega^{\mathcal{B}} \times \mathbf{b}_3) \cdot \mathbf{b}_2 = \left(\frac{m_Q}{f}\dddot{\mathbf{x}}_Q - \frac{\dot{f}}{f}\mathbf{b}_3\right) \cdot \mathbf{b}_2 = -{}^{\mathcal{I}}\Omega^{\mathcal{B}} \cdot \mathbf{b}_1 \tag{58}$$

Finally, for a Z-Y-X rotation, in Euler-angle coordinates:

$$\begin{aligned}{}^{\mathcal{I}}\Omega^{\mathcal{B}} &= {}^{\mathcal{I}}\Omega^{\mathcal{C}} + {}^{\mathcal{C}}\Omega^{\mathcal{B}} \\ &= \dot{\psi}\mathbf{e}_3 + (\dot{\theta}\mathbf{c}_2 + \dot{\phi}\mathbf{b}_1)\end{aligned} \tag{59}$$

We can use this to find:

$${}^{\mathcal{I}}\Omega^{\mathcal{B}} \cdot \mathbf{b}_2 = (\dot{\psi}\mathbf{e}_3 + \dot{\theta}\mathbf{c}_2) \cdot \mathbf{b}_2$$

$$\dot{\theta} = \frac{{}^{\mathcal{I}}\Omega^{\mathcal{B}} \cdot \mathbf{b}_2 - \dot{\psi}\mathbf{e}_3 \cdot \mathbf{b}_2}{\mathbf{c}_2 \cdot \mathbf{b}_2} \tag{60}$$

$${}^{\mathcal{I}}\Omega^{\mathcal{B}} \cdot \mathbf{b}_3 = (\dot{\psi}\mathbf{e}_3 + \dot{\theta}\mathbf{c}_2) \cdot \mathbf{b}_3 \tag{61}$$

Eqs. 57 - 61 give the body-frame components of ${}^{\mathcal{I}}\Omega_{\mathcal{B}}$.

Differentiating the equation of motion again:

$$\begin{aligned}m_Q\mathbf{x}_Q^{(4)} = \ddot{f}\mathbf{b}_3 + 2\dot{f}\left({}^{\mathcal{I}}\Omega^{\mathcal{B}} \times \mathbf{b}_3\right) \\ + f\left({}^{\mathcal{I}}\alpha^{\mathcal{B}} \times \mathbf{b}_3 + {}^{\mathcal{I}}\Omega^{\mathcal{B}} \times ({}^{\mathcal{I}}\Omega^{\mathcal{B}} \times \mathbf{b}_3)\right)\end{aligned} \tag{62}$$

Taking the $\mathbf{b}_3$ component:

$$\ddot{f} = m_Q(\mathbf{x}_Q^{(4)} \cdot \mathbf{b}_3) - 2\dot{f}\left({}^{\mathcal{I}}\Omega^{\mathcal{B}} \times \mathbf{b}_3\right) - f{}^{\mathcal{I}}\Omega^{\mathcal{B}} \times ({}^{\mathcal{I}}\Omega^{\mathcal{B}} \times \mathbf{b}_3) \tag{63}$$

We can substitute Eq. 63 back into Eq. 62 to solve for ${}^{\mathcal{I}}\alpha^{\mathcal{B}} \times \mathbf{b}_3$. We can find the $\mathbf{b}_1$ and $\mathbf{b}_2$ components of ${}^{\mathcal{I}}\alpha^{\mathcal{B}}$ as done in Eqs. 57 and 58. To find the $\mathbf{b}_3$ component, we use:

$$\begin{aligned}{}^{\mathcal{I}}\alpha^{\mathcal{B}} &= {}^{\mathcal{I}}\alpha^{\mathcal{C}} + {}^{\mathcal{I}}\Omega^{\mathcal{C}} \times {}^{\mathcal{C}}\Omega^{\mathcal{B}} + {}^{\mathcal{C}}\alpha^{\mathcal{B}} \\ &= \ddot{\psi}\mathbf{e}_3 + \dot{\psi}\mathbf{e}_3 \times (\dot{\theta}\mathbf{c}_2 + \dot{\phi}\mathbf{b}_1) \\ &\quad + (\ddot{\theta}\mathbf{c}_2 + \dot{\theta}\mathbf{c}_2 \times \dot{\phi}\mathbf{b}_1 + \ddot{\phi}\mathbf{b}_1)\end{aligned} \tag{64}$$

$${}^{\mathcal{I}}\alpha^{\mathcal{B}} \cdot \mathbf{b}_2 = (\ddot{\psi}\mathbf{e}_3 + \dot{\psi}\mathbf{e}_3 \times \dot{\theta}\mathbf{c}_2 + \ddot{\theta}\mathbf{c}_2) \cdot \mathbf{b}_2 \tag{65}$$

We can use this in Eq. 65 to solve for:

$$\ddot{\theta} = \frac{{}^{\mathcal{I}}\alpha^{\mathcal{B}} \cdot \mathbf{b}_2 - (\ddot{\psi}\mathbf{e}_3 + \dot{\psi}\mathbf{e}_3 \times \dot{\theta}\mathbf{c}_2) \cdot \mathbf{b}_2}{\mathbf{c}_2 \cdot \mathbf{b}_2} \tag{66}$$

Thus, we know all the terms needed to find:

$${}^{\mathcal{I}}\alpha^{\mathcal{B}} \cdot \mathbf{b}_3 = (\ddot{\psi}\mathbf{e}_3 + \dot{\psi}\mathbf{e}_3 \times \dot{\theta}\mathbf{c}_2 + \ddot{\theta}\mathbf{c}_2) \cdot \mathbf{b}_3 \tag{67}$$

This gives us all the body-frame components of ${}^{\mathcal{I}}\alpha^{\mathcal{B}}$, or ${}^{\mathcal{I}}\dot{\Omega}^{\mathcal{B}}_{\mathcal{B}}$.

Lastly, the moment input be found from the rotational equation of motion:

$$\mathbf{M} = {}^{\mathcal{I}}\Omega^{\mathcal{B}}_{\mathcal{B}} \times [\mathbb{I}]_{\mathcal{B}}{}^{\mathcal{I}}\Omega^{\mathcal{B}}_{\mathcal{B}} + [\mathbb{I}]_{\mathcal{B}}{}^{\mathcal{I}}\dot{\Omega}^{\mathcal{B}}_{\mathcal{B}}$$

Note that the moment input $M$ is a function of the fourth derivative of the quadrotor position.

### *B. Differential flatness of the quadrotor-with-load subsystem*

We propose $\mathbf{y}_1 = [\mathbf{x}_L \quad \psi]^T$ as the set of flat outputs for the quadrotor-with-load system, with state:

$$\mathbf{x}_1 = [\mathbf{x}_L \quad \dot{\mathbf{x}}_L \quad \mathbf{p} \quad \omega \quad {}^{\mathcal{I}}R_{\mathcal{B}} \quad {}^{\mathcal{I}}\Omega^{\mathcal{B}}_{\mathcal{B}}]^T$$

and input:

$$\mathbf{u} = [f \quad \mathbf{M}]^T$$

The load velocity and acceleration, $\dot{\mathbf{x}}_L$ and $\ddot{\mathbf{x}}_L$, are known from simple differentiation of the load position. Recall the load's equation of motion, Eq. 46 and the previously found value of $\mathbf{p}$, Eq. 47:

$$-T\mathbf{p} = m_L(\ddot{\mathbf{x}}_L + g\mathbf{e}_3)$$
$$\mathbf{p} = \frac{T\mathbf{p}}{\|T\mathbf{p}\|} = \frac{-(\ddot{\mathbf{x}}_L + g\mathbf{e}_3)}{\|\ddot{\mathbf{x}}_L + g\mathbf{e}_3\|}$$

From this, we can also find an explicit expression for the tension force:

$$T = m_L\|g\mathbf{e}_3 + \ddot{\mathbf{x}}_L\| \tag{68}$$

Differentiating the equation of motion:

$$-T\dot{\mathbf{p}} - \dot{T}\mathbf{p} = m_L\dddot{\mathbf{x}}_\mathbf{L}$$

Using $\dot{\mathbf{p}} \cdot \mathbf{p} = 0$:

$$\dot{T} = -m_L(\dddot{\mathbf{x}}_L \cdot \mathbf{p}) \tag{69}$$

$$\dot{\mathbf{p}} = \frac{-(m_L\dddot{\mathbf{x}}_L + \dot{T}\mathbf{p})}{T} \tag{70}$$

Notice that:

$$\dot{\mathbf{p}} = \omega \times \mathbf{p}$$
$$\dot{\mathbf{p}} \times \mathbf{p} = (\omega \times \mathbf{p}) \times \mathbf{p}$$
$$= -\mathbf{p} \times (\omega \times \mathbf{p})$$
$$= \mathbf{p}(\omega \cdot \mathbf{p}) - \omega(\mathbf{p} \cdot \mathbf{p})$$
$$= -\omega$$

Using Eq. 70:

$$\omega = \frac{(m_L\dddot{\mathbf{x}}_L + \dot{T}\mathbf{p})}{T} \times \mathbf{p}$$
$$= \frac{m_L\dddot{\mathbf{x}}_L}{T} \times \mathbf{p} \tag{71}$$

Next, since $\mathbf{p}$ is known, we can also find:

$$\mathbf{x}_Q = \mathbf{x}_L - l\mathbf{p}$$

Through continued differentiation of the equation of motion for the load, we can find the higher derivatives of $\mathbf{p}$ and thus the higher derivatives of $\mathbf{x}_Q$. With these derivatives of $\mathbf{x}_Q$ and the derivatives of $\mathbf{x}_L$ from the flat outputs, we can derive the quadrotor attitude states and inputs in a manner similar to that in Section IV-A. The complete derivation is found in Appendx B. In particular, note that the moment $M$ input is a function of sixth derivative of the load position.

## V. Planar model

We now approximate the system as a planar system operating in the $y - z$ plane, as illustrated in Fig. 3. While this simplification does not represent the full system, it serves as an important first step towards understanding the challenges in working with the full hybrid system and developing an intuition for the usable techniques.

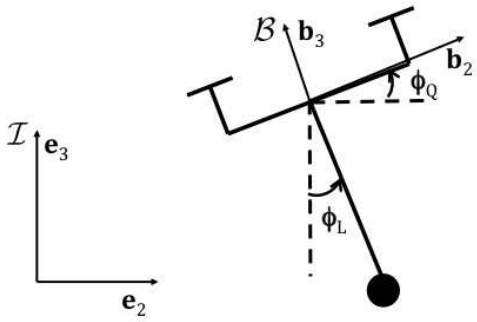


Fig. 3: Planar quadrotor with a point-mass load

We parametrize the quadrotor attitude with angle $\phi_Q$ and the load orientation with angle $\phi_L$, and specialize the angular state variables to the plane in terms of these variables:

$$[\mathbb{I}]_{\mathcal{B}} = \begin{bmatrix} J_Q & 0 & 0 \\ 0 & 0 & 0 \\ 0 & 0 & 0 \end{bmatrix}$$
$${}^{\mathcal{I}}\mathbf{R}_{\mathcal{B}} = \begin{bmatrix} 1 & 0 & 0 \\ 0 & \cos(\phi_Q) & -\sin(\phi_Q) \\ 0 & \sin(\phi_Q) & \cos(\phi_Q) \end{bmatrix}, {}^{\mathcal{I}}\Omega^{\mathcal{B}}_{\mathcal{B}} = \begin{bmatrix} \dot{\phi}_Q & 0 & 0 \end{bmatrix}^T$$
$$\mathbf{p} = \begin{bmatrix} 0 & \sin(\phi_L) & -\cos(\phi_L) \end{bmatrix}^T, \omega = \begin{bmatrix} \dot{\phi}_L & 0 & 0 \end{bmatrix}^T$$
$$\mathbf{M} = \begin{bmatrix} M & 0 & 0 \end{bmatrix}^T$$

Substituting these variables into the the equations of motion, Eqs. 8 - 13 and Eqs. 38 - 43, and taking non-zero components gives the planar dynamical equations for the system. For subsystem 1, this results in the equations:

$$(m_Q + m_L)(\ddot{\mathbf{x}}_L + g\mathbf{e}_3) = (-f\cos(\phi_Q - \phi_L) - m_Q l\dot{\phi}_L^2)\mathbf{p} \tag{72}$$

$$m_Q l\ddot{\phi}_L = f\sin(\phi_Q - \phi_L) \tag{73}$$

$$J_Q\ddot{\phi}_Q = M \tag{74}$$

For subsystem 2, we obtain:

$$\ddot{\mathbf{x}}_L + g\mathbf{e}_3 = 0 \tag{75}$$

$$m_Q(\ddot{\mathbf{x}}_Q + g\mathbf{e}_3) = f\mathbf{b}_3 = f\begin{bmatrix}-\sin(\phi_Q) & \cos(\phi_Q)\end{bmatrix}^T \tag{76}$$

$$J_Q\ddot{\phi}_Q = M \tag{77}$$

Here, we have redefined the variables as given in Table II. Note the slight abuse of notation, where we retain the same variable names but alter their domains for the planar model.

TABLE II: Variables of the planar dynamic model

| | |
|---|---|
| $J_Q \in \mathbb{R}$ | Inertia of quadrotor |
| $f, M \in \mathbb{R}$ | Magnitude of thrust, moment on quadrotor |
| $\mathbf{x}_Q, \mathbf{x}_L \in \mathbb{R}^2$ | Position vector of quadrotor, load, in $\mathcal{I}$ |
| $\mathbf{p} \in \mathbb{S}^1$ | Unit vector from quadrotor to load |
| $\mathbf{R} \in SO(2)$ | Rotation matrix of quadrotor from $\mathcal{B}$ to $\mathcal{I}$ |
| $\mathcal{I}$ | Intertial frame, axes $\mathbf{e}_2$, $\mathbf{e}_3$ |
| $\mathcal{B}$ | Quadrotor body frame, axes $\mathbf{b}_2$, $\mathbf{b}_3$ |
| $\phi_Q \in (-\pi, \pi]$ | Angle of quadrotor counter-clockwise from horizontal |
| $\phi_L \in (-\pi, \pi]$ | Angle of load counter-clockwise from vertical |
| $\dot{\phi_Q}, \dot{\phi_L} \in \mathbb{R}$ | Angular velocity of the quadrotor, load |

The new states for the planar quadrotor-with-load and quadrotor subsystems become:

$$\mathbf{x}_1 = [\mathbf{x}_L \;\; \dot{\mathbf{x}}_L \;\; \phi_L \;\; \dot{\phi}_L \;\; \phi_Q \;\; \dot{\phi}_Q]^T$$
$$\mathbf{x}_2 = [\mathbf{x}_L \;\; \dot{\mathbf{x}}_L \;\; \mathbf{x}_Q \;\; \dot{\mathbf{x}}_Q \;\; \phi_Q \;\; \dot{\phi}_Q]^T,$$

with configuration manifolds, $\mathbb{S}^1 \times SE(2)$ and $\mathbb{R}^2 \times SE(2)$, respectively.

The guards remain the same and the resets become:

$$\mathcal{R} = \{R_{(1,2)} = [\mathbf{x}_L \;\; \dot{\mathbf{x}}_L \;\; \mathbf{x}_L - l\mathbf{p} \;\; \dot{\mathbf{x}}_L - l\dot{\mathbf{p}} \;\; \phi_Q \;\; \dot{\phi}_Q]^T$$
$$R_{(2,1)} = [\mathbf{x}_L \;\; \dot{\mathbf{x}}_Q \;\; \cos^{-1}(\frac{\mathbf{x}_Q - \mathbf{x}_L}{l} \cdot \mathbf{e}_3) \;\; 0 \;\; \phi_Q \;\; \dot{\phi}_Q]^T\}\}$$

The differential flatness properties of the system continue to apply in the planar case. However, iince the yaw angle is constrained to 0, the flat outputs are simply $\mathbf{y}_1 = [\mathbf{x}_L]^T$ and $\mathbf{y}_2 = [\mathbf{x}_Q]^T$. We can again substitute the planar specializations of the angular variables into the previously derived differential flatness equations.

From this point onwards, we will work exclusively with the planar system model.

## VI. Control Design

Next, we design system's controllers. In particular, we want to be able to track the flat outputs of each subsystem.

### A. Quadrotor subsystem

In the quadrotor system, we use a planar adaptation of the nonlinear geometric controller proposed by Lee et al. [15]. Fig. 7 illustrates the nested structure of the controller. The inner loop controller tracks a given desired attitude angle through its output commanded moment. The outer loop tracks a desired quadrotor position by outputting a commanded thrust and desired attitude angle.

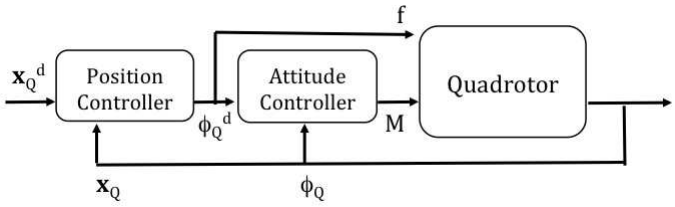


Fig. 4: Structure of the quadrotor position controller

*1) Attitude controller:* For attitude errors be $e_Q = \phi_Q - \phi_Q^d$, $\dot{e}_Q = \dot{\phi}_Q - \dot{\phi}_Q^d$, let the commanded moment be:

$$M^d = J_Q(-K_{p_{\phi_Q}}(e_Q) - K_{d_{\phi_Q}}(\dot{e}_Q) + \ddot{\phi}_Q^d) \tag{78}$$

This control law is exponentially stable about the origin of the error state, $\mathbf{z}_Q = [e_Q \;\; \dot{e}_Q]^T$. To see this, we first find the error dynamics from the equation of motion:

$$\ddot{e}_Q = \ddot{\phi}_Q - \ddot{\phi}_Q^d = \frac{M^d}{J_Q} - \ddot{\phi}_Q^d \tag{79}$$

Using $\mathbf{M}$ as defined by the control law:

$$\begin{aligned}\ddot{e}_Q &= \frac{J_Q(-K_{p_{\phi_Q}}(e_Q) - K_{d_{\phi_Q}}(\dot{e}_Q) + \ddot{\phi}_Q^d)}{J_Q} - \ddot{\phi}_Q^d \\ &= -K_{p_{\phi_Q}}(e_Q) - K_{d_{\phi_Q}}(\dot{e}_Q)\end{aligned} \tag{80}$$

The error dynamics become:

$$\ddot{\mathbf{z}}_Q = \begin{bmatrix}0 & 1 \\ -K_{p_{\phi_Q}} & -K_{d_{\phi_Q}}\end{bmatrix}\mathbf{z}_Q \tag{81}$$

This is a linear time-invariant system, with eigenvalues:

$$\lambda = \frac{1}{2}(-b \pm \sqrt{b^2 - 4a}), a = K_{p_{\phi_Q}}, b = K_{d_{\phi_Q}}$$

$\lambda$ will have negative real part for all $K_{p_{\phi_Q}} > 0$ and $K_{d_{\phi_Q}} > 0$. Thus, the origin of the error state $[e_Q \;\; \dot{e}_Q]^T$ is exponentially stable.

*2) Position controller:* Next, we design the outer loop controller that tracks a desired quadrotor position, $\mathbf{x}_Q^d$. For error terms $\mathbf{e}_x = \mathbf{x}_Q - \mathbf{x}_Q^d$, $\dot{\mathbf{e}}_x = \dot{\mathbf{x}}_Q - \dot{\mathbf{x}}_Q^d$, let the input thrust be calculated with:

$$\mathbf{F}^d = -K_p\mathbf{e}_x - K_d\dot{\mathbf{e}}_x + m_Q(g\mathbf{e}_3 + \ddot{\mathbf{x}}_Q^d) \tag{82}$$

$$f^d = \mathbf{F}^d \cdot \mathbf{b}_3 \tag{83}$$

Furthermore, we define the desired attitude as:

$$\mathbf{b}_3^d = \frac{\mathbf{F}^d}{\|\mathbf{F}^d\|} \tag{84}$$

$$\phi_Q^d = \tan^{-1}\left(\frac{-\mathbf{b}_3^d \cdot \mathbf{e}_2}{\mathbf{b}_3^d \cdot \mathbf{e}_3}\right) \tag{85}$$

We have shown in the previous section that the attitude dynamics are exponentially stable. By the Converse Lyapunov Theorem, there exists a Lyapunov function $V_Q$ such that for positive definite matrices $M_q$, $M_Q$, and $W_Q$ and all $\mathbf{z}_Q$:

$$\mathbf{z}_Q^T M_q \mathbf{z}_Q \leq V_Q \leq \mathbf{z}_Q^T M_Q \mathbf{z}_Q \tag{86}$$

$$\dot{V}_Q \leq -\mathbf{z}_Q^T W_Q \mathbf{z}_Q \tag{87}$$

Assume the initial attitude and position errors and the desired acceleration are uniformly bounded with:

$$|e_Q(0)| < \frac{\pi}{2}$$
$$\|\mathbf{e}_x(0)\| < \mathbf{e}_{x,max}$$
$$\|m_Q(g\mathbf{e}_3 + \ddot{\mathbf{x}}_Q^d)\| \leq Y$$

Consider $W_Q$ defined in Eq. 87 and additionally define:

$$W_{xQ} = \begin{bmatrix} \frac{cY}{m_Q} & 0 \\ Y + \mathbf{e}_{x,max} & 0 \end{bmatrix} \tag{88}$$

$$W_x = \begin{bmatrix} \frac{cK_p}{m_Q}(1-\alpha) & \frac{1}{2}\frac{cK_d}{m_Q}(1-\alpha) \\ \frac{1}{2}\frac{cK_d}{m_Q}(1-\alpha) & K_d(1-\alpha) - c \end{bmatrix} \tag{89}$$

Assume the existence of positive constants $c, \alpha, K_p, K_d$ satisfying the conditions:

$$c < \min\left\{\sqrt{m_Q K_p}, K_d(1-\alpha), \frac{4m_Q K_p K_d(1-\alpha)}{4m_Q K_p + K_d^2(1-\alpha)}\right\}, \tag{90}$$

$$\lambda_m(W_x) > \frac{\|W_{xQ}\|^2}{4\lambda_m(W_Q)}, \tag{91}$$

where $\lambda_m$ indicates the minimum eigenvalue. Then, the quadrotor position error dynamics are exponentially stable about the origin.

Additionally define the notion of exponential attractiveness: an equilibrium point $\mathbf{x} = 0$ is exponentially attractive if for some $\delta > 0$, there exists constants $\gamma(\delta) > 0$ and $\beta > 0$ such that $\|\mathbf{x}(0)\| < \delta$ implies $\|\mathbf{x}(t)\| \leq \gamma(\delta)e^{-\beta t}$ for all $t > 0$ [15]. If the initial attitude error $|e_Q(0)| \geq \frac{\pi}{2}$ but all other conditions hold, then the quadrotor position error dynamics are exponentially attractive.

This proof is provided in Appendix C.

### *B. Quadrotor-with-load subsystem*

For the planar quadrotor-with-load subsystem, we use the controller proposed by Sreenath et al. [30], which we briefly describe here. The controller structure is illustrated in Fig. 8. Note the similar structure to the quadrotor subsystem controller.

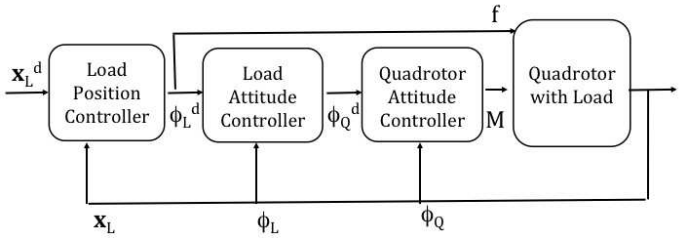


Fig. 5: Structure of the load position controller

The quadrotor attitude controller remains the same as in the quadrotor subsystem. For load attitude errors as $e_L = \phi_L^d - \phi_L$, $\dot{e}_L = \dot{\phi}_L - \dot{\phi}_L^d$, the load attitude control law is:

$$\phi_Q^d = \phi_L + \sin^{-1}\left(-k_{p_{\phi_L}} e_L - k_{d_{\phi_L}} \dot{e}_L + \frac{\phi_L^d m_Q l}{f}\right), \tag{92}$$

Assume $k_{p_{\phi_L}} > 0$, $k_{d_{\phi_L}} > 0$ and the initial conditions satisfy:

$$\| - k_{p_{\phi_L}} e_L - k_{d_{\phi_L}} \dot{e}_L + \frac{\ddot{\phi}_L^d m_Q l}{f}\| < 1 \tag{93}$$

Further, assume the existence of positive constants $\alpha, c_1, k_{p_{\phi_L}}$, and $k_{d_{\phi_L}}$ where:

$$0 < \frac{f}{m_Q l} \leq \alpha$$
$$c_1 < \min\left\{\sqrt{\alpha k_{p_{\phi_L}}}, \frac{k_{p_{\phi_L}} k_{d_{\phi_L}}}{k_{p_{\phi_L}} + k_{d_{\phi_L}}/2}\right\}$$
$$W_L = \begin{bmatrix} \alpha k_{p_{\phi_L}} c_1 & \frac{\alpha k_{d_{\phi_L}} c_1}{2} \\ \frac{\alpha k_{d_{\phi_L}} c_1}{2} & \alpha k_{d_{\phi_L}} - c_1 \end{bmatrix}$$
$$W_{LQ} = \begin{bmatrix} c_1\alpha^2 & \alpha^2 \\ 0 & 0 \end{bmatrix}$$
$$\lambda_m(W_L) > \frac{\|W_{LQ}\|^2}{4\lambda_m(W_Q)}$$

The outermost load position controller is defined with respect to $\mathbf{e}_x = \mathbf{x}_L - \mathbf{x}_L^d$, $\dot{\mathbf{e}}_x = \dot{\mathbf{x}}_L - \dot{\mathbf{x}}_L^d$ as:

$$f^d = (A + B) \cdot \mathbf{b}_3 \tag{94}$$
$$A = -k_p \mathbf{e}_x - k_d \dot{\mathbf{e}}_x + (m_L \ddot{\mathbf{x}}_L^d + m_L g \mathbf{e}_3) \tag{95}$$
$$B = m_L \ddot{\mathbf{x}}_L^d - m_Q l \ddot{\mathbf{p}}_L^d + m_Q g \mathbf{e}_3 \tag{96}$$

Furthermore, we can define:

$$\mathbf{p}^d = -\frac{A}{\|A\|}$$
$$\phi_L^d = \tan^{-1}\left(\frac{-A \cdot \mathbf{e}_2}{A \cdot \mathbf{e}_3}\right) \tag{97}$$

Assume the uniform bound:

$$\|m_L(\ddot{\mathbf{x}}_L^d + g\mathbf{e}_3) + m_Q(\ddot{\mathbf{x}}_Q^d + g\mathbf{e}_3)\| \leq C$$

and the existence of positive constants $d_1, d_2, c_2, k_p$, and $k_d$ such that:

$$0 < \frac{1}{|\mathbf{p}^d \cdot R\mathbf{e}_3|} \leq |e_L + e_Q| \leq \beta \leq 1$$
$$m_Q l \|\ddot{\mathbf{p}} - \ddot{\mathbf{p}}^d\| \leq d_1|e_L| + d_2|\dot{e}_L|$$
$$c_2 < \min\left\{\sqrt{k_p}, \frac{k_p k_d(1+\beta)^2}{k_p + k_d^2/4}\right\}$$

With this controller, the load position error exponentially converges to 0. The proofs for the stability properties of Eqs. 92 - 97 is found in Sreenath et al. [30].

## VII. Trajectory Generation

Now that we have derived and designed controllers for tracking the flat outputs of each subsystem, we can plan their trajectories in the flat output space. Note that, assuming a Euler-angle parametrization of the rotation matrix, the dimension of the full state for both subsystems is 18, while their flat output spaces are dimension 2. This reduction of dimensionality is a clear advantage of planning in this space.

### A. Trajectory optimization

In this section, we describe a general method for trajectory optimization. This method has been described in a number of previous works [19], [21], [25] and proven effective for generating smooth and fast trajectories for quadrotor systems.

The trajectory generation problem can be stated as: given a series of $n_w$ waypoint constraints, each dictating a desired position or higher derivative value at a specified time, find a trajectory $x(t)$ that satisfies the constraints while minimizing the cost functional:

$$J = \int_{t_0}^{t_1} \| \frac{d^r x(t)}{dt} \|^2 dt \tag{98}$$

Let $P_i(t)$, for $i = 1, 2, ..., N$, be a set of basis functions. We write the trajectory as $x(t) = c_0 + \sum_{i=1}^{N} c_i P_i(t)$. Defining the vector $\mathbf{c} = [c_0 \;\; c_1 \;\; c_2 \;\; ... \;\; c_N]^T$, we can formulate the problem as the Quadratic Program (QP):

$$\begin{aligned} &\text{minimize } J = \mathbf{c}^T Q \mathbf{c} \\ &\text{subject to } A\mathbf{c} = \mathbf{b} \end{aligned} \tag{99}$$

Here, $Q$ is a symmetric, square matrix found by explicitly evaluating the cost functional integral in terms of the trajectory coefficients. The constraint function $A\mathbf{c} = \mathbf{b}$ comes from the waypoint constraints. Since the problem only has equality constraints, Eq. 99 has a known analytic solution:

$$\begin{bmatrix} 2Q & A^T \\ A & 0 \end{bmatrix} \begin{bmatrix} \mathbf{c} \\ \lambda \end{bmatrix} = \begin{bmatrix} \mathbf{0} \\ \mathbf{b} \end{bmatrix},$$

where $\lambda$ is a vector of Lagrange multipliers. Alternatively, numerical tools such as Matlab can also be used.

Now suppose the trajectory were an n-dimensional vector, $\mathbf{x}(t) = [x_1(t) \;\; x_2(t) \;\; ... \;\; x_n(t)]^T$. If the waypoint constraints are independent, then each component of $x$ can be optimized independently. Otherwise, we simply concatenate the coefficients to form the variable vector $\mathbf{c} = [c_{0,x_1} \;\; c_{1,x_1} \;\; ... \;\; c_{N,x_n}]^T$.

Mellinger and Kumar [19], [21] show that since the input moment is a function of the fourth derivative of the quadrotor position, finding minimum-snap trajectories, or $r = 4$ in Eq. 98, yields smooth trajectories through all waypoint constraints. We apply the same reasoning to our system. In the quadrotor subsystem, we seek $\mathbf{x}(t) = \mathbf{x}_Q^d(t)$ and minimize the fourth derivative of the quadrotor trajectory. In the quadrotor-with-load subsystem, where $\mathbf{x}(t) = \mathbf{x}_L^d(t)$, we minimize the sixth derivative of the load trajectory (since the input moment is a function of the sixth derivative of the load position).

### B. Formulation with trigonometric basis

The technique presented in Section VII-A applies for any family basis functions $P_i(t)$. A popular choice for quadrotors has been polynomial functions $P_i(t) = t^i$ [19], [25]. Mellinger et al. [21] alternatively use Legendre polynomials.

Unlike previous work, we chose instead to use a trigonometric basis, with trajectories of the form:

$$x(t) = c_0 + \sum_{n=1}^{N} A_n \cos(\frac{2n\pi t}{L}) + \sum_{m=1}^{M} B_m \sin(\frac{2m\pi t}{L}), \tag{100}$$

where the period $L$ is chosen *a priori*. In particular, trigonometric functions are periodic and thus well-suited for a repeated maneuver like the load-transport maneuver. In addition, $\sin()$ and $\cos()$ are $C^\infty$ differentiable, the trajectory is guaranteed to be smooth. Finally, trigonometric functions have desirable orthogonality properties, allowing us to simplify the matrix $Q$ in the quadratic form of the cost functional to a simple diagonal matrix.

To specialize the QP in Eq. 99 for a trigonometric basis, we analytically evaluate the cost function integral. For any derivative $r$, where $r \geq 0$:

$$\begin{aligned} x^{(r)}(t) = c_0^{(r)} &+ \sum_{n=1}^{N} A_n (\frac{2n\pi}{L})^r \cos(\frac{2n\pi}{L}t + \frac{r\pi}{2}) \\ &+ \sum_{m=1}^{M} B_m (\frac{2m\pi}{L})^r \sin(\frac{2m\pi}{L}t + \frac{r\pi}{2}) \end{aligned} \tag{101}$$

The cost functional, Eq. 98, becomes:

$$\begin{aligned} J &= \int_0^L \| \frac{d^r x(t)}{dt} \|^2 dt \\ &= \int_0^L \left( c_0^{(r)} + \sum_{n=1}^{N} A_n (\frac{2n\pi}{L})^r \cos(\frac{2n\pi}{L}t + \frac{r\pi}{2}) \right. \\ &\qquad \left. + \sum_{m=1}^{M} B_m (\frac{2m\pi}{L})^r \sin(\frac{2m\pi}{L}t + \frac{r\pi}{2}) \right)^2 dt \\ &= \int_0^L (c_0^{(r)})^2 + \sum_{n=1}^{N} A_n^2 (\frac{2n\pi}{L})^{2r} \cos^2(\frac{2n\pi}{L}t + \frac{r\pi}{2}) \\ &\quad + \sum_{m=1}^{M} B_m^2 (\frac{2m\pi}{L})^{2r} \sin^2(\frac{2m\pi}{L}t + \frac{r\pi}{2}) \\ &\quad + 2c_0^{(r)} (\sum_{n=1}^{N} A_n (\frac{2n\pi}{L})^r \cos(\frac{2n\pi}{L}t + \frac{r\pi}{2}) \\ &\qquad + \sum_{m=1}^{M} B_m (\frac{2m\pi}{L})^r \sin(\frac{2m\pi}{L}t + \frac{r\pi}{2})) \\ &\quad + 2 \sum_{n=1}^{N} \sum_{p=n}^{N} A_n A_p (\frac{2n\pi}{L})^r (\frac{2p\pi}{L})^r \\ &\qquad \cos(\frac{2n\pi}{L}t + \frac{r\pi}{2}) \cos(\frac{2p\pi}{L}t + \frac{r\pi}{2}) \\ &\quad + 2 \sum_{n=1}^{N} \sum_{m=1}^{M} A_n B_m (\frac{2n\pi}{L})^r (\frac{2m\pi}{L})^r \\ &\qquad \cos(\frac{2n\pi}{L}t + \frac{r\pi}{2}) \sin(\frac{2m\pi}{L}t + \frac{r\pi}{2}) \\ &\quad + 2 \sum_{m=1}^{M} \sum_{p=m}^{M} B_m B_p (\frac{2m\pi}{L})^r (\frac{2p\pi}{L})^r \\ &\qquad \sin(\frac{2m\pi}{L}t + \frac{r\pi}{2}) \sin(\frac{2p\pi}{L}t + \frac{r\pi}{2}) dt \end{aligned}$$

Assume $r > 0$. Thus, $c_0^{(r)} = 0$. We can use orthogonality

properties:

$$\int_0^L \cos(\frac{2n\pi}{L}t)\sin(\frac{2m\pi}{L}t)dt = 0$$

$$\int_0^L \cos(\frac{2n\pi}{L}t)\cos(\frac{2m\pi}{L}t)dt = \begin{cases} L, & n=m=0 \\ \frac{L}{2}, & n=m>0 \\ 0, & n\neq m \end{cases}$$

$$\int_0^L \sin(\frac{2n\pi}{L}t)\sin(\frac{2m\pi}{L}t)dt = \begin{cases} \frac{L}{2}, & n=m>0 \\ 0, & n\neq m \text{ or } n=m=0 \end{cases},$$

to reduce the cost functional to the simple form:

$$J = \sum_{n=1}^{N} A_n^2(\frac{2n\pi}{L})^{2r}(\frac{L}{2}) + \sum_{m=1}^{M} B_m^2(\frac{2m\pi}{L})^{2r}(\frac{L}{2})$$

Let $\mathbf{c} = [c_0 \quad A_1 \quad A_2 \quad ... \quad A_N \quad B_1 \quad B_2 \quad ... \quad B_M]^T$. In the quadratic form of $J$, $Q$ becomes:

$$Q[i,j] = \begin{cases} 0, & i\neq j \text{ or } i=j=1 \\ \frac{L}{2}(\frac{2i\pi}{L})^{2r}, & i=j\leq N \\ \frac{L}{2}(\frac{2(i-N-1)\pi}{L})^{2r}, & N<i=j\leq(N+M+1) \end{cases} \tag{102}$$

Note that we index the elements of $Q$ from 1. Finally, for $r = 0$:

$$J = c_0^2 L + \sum_{n=1}^{N} A_n^2(\frac{2n\pi}{L})^{2r}(L)$$

$$Q[i,j] = \begin{cases} 0, & i\neq j \text{ or } i=j=1 \\ L(\frac{2i\pi}{L})^{2r}, & i=j\leq N \\ 0, & N<i=j\leq(N+M+1) \end{cases}$$

The derivative expression in Eq. 101 also allows us to express a waypoint constraint on any derivative at time $t_i$ as a linear equation of the coefficients. This allows us to easily construct the constraint function $A\mathbf{c} = \mathbf{b}$.

For each problem, we must also choose the period $L$ and the number of coefficients $N$ and $M$. Suppose we have a series of waypoint constraints whose corresponding times are over $[t_0, t_f]$. We choose $L \geq (t_f - t_0)$. Since the trajectory is periodic, the equality is only possible if all waypoint constraints at $t_0$ are the same as those at $t_f$. For $n_w$ constraints, the chosen number of coefficients must satisfy $(N + M + 1) \geq n_w$. However, special consideration must be given to constraints at times where $\sin()$ or $\cos()$ are 0. For example, for two position constraints each at $t = 0$ and $t = \frac{L}{2}$, we must specifically have $(N+1) \geq 2$, since $\sin(\frac{2m\pi}{L}t)$ disappears. In general, we must also satisfy $(N+1) \geq n_p$, $N \geq n_e$, and $M \geq n_0$, where $n_p$, $n_e$, and $n_o$ are the number of constraints on position, even derivatives, and odd derivatives, respectively, at $t = 0, \frac{L}{2}, L$.

### C. Trajectory design for the load-transport maneuver

Finally, we use the previously described methods to design trajectories for the load-transport maneuver. Unlike previous works, which generated trajectories for a single dynamical system, we wish to design trajectories for the full hybrid system. In particular, this involves planning the location of switches between subsystems and designing subsystem trajectories that will transition continuously at these switching points.

Let the load begin at position $(y_0, z_0)$ and have desired ending position $(y_1, z_1)$. We begin by designing the desired load trajectory, $\mathbf{x}_L^d(t) = [y_L^d(t) \quad z_L^d(t)]^T$. We assume that the load will be released at time $\frac{L}{2}$, which becomes the location of the switch from the quadrotor-with-load to the quadrotor subsystem. Defining the switching time in terms of $L$ allows us to find the trajectory coefficients without explicitly defining $L$, which will be chosen later.

Suppose the load is released at $(y_r, z_r)$ with velocity $(\dot{y}_r, \dot{z}_r)$. This gives the boundary conditions:

$$\mathbf{x}_L^d(0) = [y_0 \quad z_0]^T$$
$$\mathbf{x}_L^d\left(\frac{L}{2}\right) = [y_r \quad z_r]^T$$
$$\dot{\mathbf{x}}_L^d\left(\frac{L}{2}\right) = [\dot{y}_r \quad \dot{z}_r]^T$$

However, the release positions and velocities cannot be chosen independently, as the load must travel the required horizontal distance in the time it takes to fall to the ground. This constraint is characterized with:

$$y_1 - y_r = \dot{y}_r\tau \tag{103}$$
$$z_1 - z_r = -\frac{g}{2}\tau^2 + \dot{z}_r\tau \tag{104}$$

Solving the previous two equations for $\tau$ and equating them gives the constraint:

$$\frac{y_1 - y_r}{\dot{y}_r} = \frac{\dot{z}_r + \sqrt{\dot{z}_r^2 - 2g(z_1 - z_r)}}{g} \tag{105}$$

This constraint is nonlinear, which is not directly usable in the QP formulation. However, if $\dot{y}_r$ is specified, Eq. 103 can be used to solve for $\tau$. This can be substituted into Eq. 104, which is a linear constraint that can be used in the QP. The analogous situation holds if $\dot{z}_r$ is specified.

However, alternatively, we limit the number of trajectory coefficients to the minimum. This allows us to find an analytical solution.

Suppose we have a trajectory of the form:

$$\mathbf{x}_L^d(t) = \begin{bmatrix} c_y + A_y\cos(\frac{2\pi t}{L}) + B_y\sin(\frac{2\pi t}{L}) \\ c_z + A_z\cos(\frac{2\pi t}{L}) + B_z\sin(\frac{2\pi t}{L}) \end{bmatrix} \tag{106}$$

Substituting this generic form into the constraint equations, we have:

$$c_y + A_y = y_0,\ c_y - A_y = y_r$$
$$c_z + A_z = z_0,\ c_z - A_z = z_r$$
$$-\frac{2\pi}{L}B_y = \dot{y}_r$$
$$-\frac{2\pi}{L}B_z = \dot{z}_r$$

Solving these and using Eq. 105:

$$c_y = \frac{y_0 + y_r}{2},\ A_y = \frac{y_0 - y_r}{2}$$
$$c_z = \frac{z_0 + z_r}{2},\ A_z = \frac{z_0 - z_r}{2}$$
$$B_z = -\frac{L}{2\pi}\dot{z}_r$$
$$B_y = (y_r - y_1)\frac{L}{2\pi}\tau, \text{where } \tau = \frac{\dot{z}_r + \sqrt{\dot{z}_r^2 - 2g(z_1 - z_r)}}{g}$$

We can then design trajectories by choosing the parameters $(y_r, z_r)$, $(\dot{y}_r, \dot{z}_r)$. For example, if we choose $y_r = y_1$, $\dot{y}_r = 0$, and an arbitrary non-zero $\dot{z}_r$, the load trajectory that is an ellipse in the $yz$-plane, where the load is released at 0 velocity directly above its desired position. Note, however, that while the load simply falls straight down, the trajectory can still be aggressive in the sense that the load angle at the time of the drop can be large.

Next, we must choose the period of the trajectory $L$, where a smaller $L$ will result in a more aggressive trajectory, that is, larger load and quadrotor angles and velocities. Rather than choosing $L$ arbitrarily, we can give it a physical meaning. From differential flatness equations, the load angle is related to the load acceleration with:

$$\tan(\phi_L) = \frac{\ddot{y}_L}{-(\ddot{z}_L + g)}$$

We choose a load angle at the time of release as $\phi_{L,r}$, which will occur at $t = \frac{L}{2}$. We can then solve:

$$\begin{aligned}\tan(\phi_{L,r}) &= \frac{\ddot{y}_L(\frac{L}{2})}{-(\ddot{z}_L(\frac{L}{2}) + g)} \\ &= \frac{-\left(\frac{2\pi}{L}\right)^2 A_y}{-\left(\left(\frac{2\pi}{L}\right)^2 A_z + g\right)} \\ L &= 2\pi\left(\frac{g\tan(\phi_{L,r})}{A_y - A_z\tan(\phi_{L,r})}\right)^{-\frac{1}{2}}\end{aligned}$$

Note that $\phi_{L,r}$ is the maximum nominal load angle for the load trajectory. The actual desired load angles, however, which are designated by the load position controller, will almost always reach values greater than this. Thus, $\phi_{L,r}$ is merely an approximation of the maximum load angle to aid in choosing $L$ with a physical intuition, not an absolute maximum for the load angle in the designed trajectory.

Finally, must design the corresponding quadrotor trajectory. To guarantee transition continuity, we again take advantage of the differential flatness of the system. We use the nominal quadrotor trajectory corresponding to the designated load trajectory as the desired trajectory for the quadrotor subsystem. The differential flatness equations of the quadrotor-with-load subsystem allows us to explicitly find the desired quadrotor trajectory as:

$$\begin{aligned}\mathbf{x}_Q^d(t) &= \mathbf{x}_L^d(t) - l\mathbf{p} \\ &= \mathbf{x}_L^d(t) + l\frac{(\ddot{\mathbf{x}}_L^d(t) + g\mathbf{e}_3)}{\|\ddot{\mathbf{x}}_L^d(t) + g\mathbf{e}_3\|}\end{aligned} \tag{107}$$

This choice of $\mathbf{x}_Q^d(t)$ guarantees that the quadrotor's trajectory will remain continuous during the load-drop transition, even if the transition does not occur exactly at $t = \frac{L}{2}$ because of system errors. After the load is released, the quadrotor simply "continues on" in its path. At time $t = L$, it will return to the states necessarily to pick up a second load at the same location. While Eq. 107 might not always be notationally simple, in implementation, we can calculate $\mathbf{x}_Q^d(t)$ at each time $t$ using the designed load trajectory and Eq. 107.

## VIII. Experimental Results

### A. Platform

We run experiments on a Hummingbird quadrotor from Ascending Technologies [1]. The quadrotor has a wingspan of 55cm and height of 8cm. To manipulate the load, we use an electromagnet whose power source can be switched on or off as needed. The magnet is suspended from a 40cm ball-chain cable. The total mass of the quadrotor, with this added mechanism, is 687g. The load is a plastic box with side length 5.7cm and mass 88g, and the top of the box is metal for attachment of the electromagnet. A VICON motion capture system [34] provides state information at 100Hz. The load is treated as a point-mass; we track the position of its center and ignore its orientation. Fig. 6 pictures our set-up.

Fig. 6: Hummingbird quadrotor with cable-suspended load

### B. Individual controllers

First, we test the controllers of each individual subsystem. Fig. 7 demonstrates the quadrotor tracking an ellipse. We see that the quadrotor controller drives errors quickly towards 0.

Next, use the trajectory optimization technique described in Section VII-B to generate a trajectory through four waypoints: $\mathbf{x}_L^d(0) = [-1.2 \quad 0.8]^T, \mathbf{x}_L^d(1.4) = [-1 \quad 1.2]^T, \mathbf{x}_L^d(2.4) = [0.3 \quad 1.5]^T, \mathbf{x}_L^d(3.2) = [1 \quad 1.4]^T, \mathbf{x}_L^d(6) = [-1.2 \quad 0.8]^T$. All higher derivatives are constrained to be 0 at $t = 0$ and $t = 6$. We choose $L = 6$, $N = 10$, $M = 5$. Fig. 8a displays the quadrotor and load trajectories, as well as the desired waypoints; Fig. 8 shows the tracking results.

### C. Load transport maneuver

Finally, we execute an example of the load transport maneuver. For the first, the parameters are: $(y_0, z_0) =$

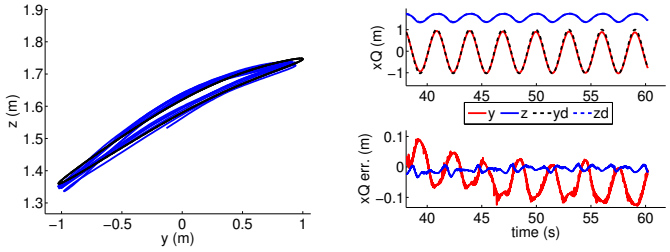


(a) 2D position




(b) Quadrotor position

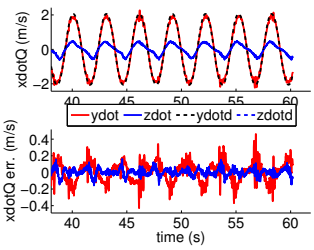


(c) Quadrotor velocity

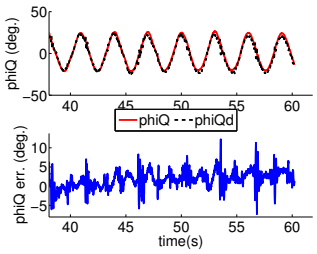


(d) Quadrotor attitude

Fig. 7: Quadrotor states over time, tracking with quadrotor subsystem controller

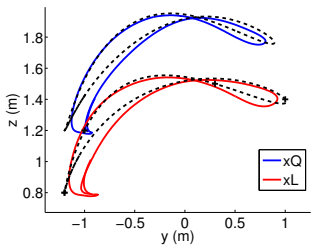


(a) 2D position

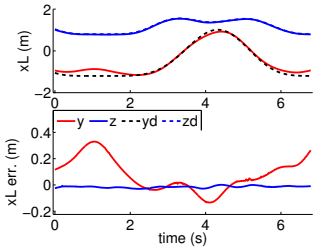


(b) Load position

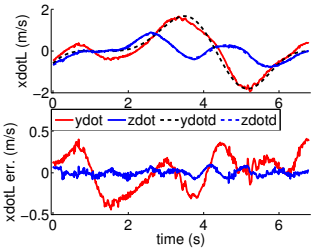


(c) Load velocity

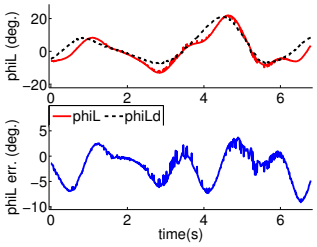


(d) Load angle

Fig. 8: Load states over time, tracking with quadrotor-with-load subsystem controller

$(-0.80, 0.81), (y_1, z_1) = (1, 0), (y_r, z_r) = (y_1, 1.2), \dot{y}_r = 0, \phi_{L,r} = 20^o$. The resulting load trajectory designed is:

$$L = 3.2840$$
$$\mathbf{x}_L^d(t) = \begin{bmatrix} 0.0953 - 0.9046\cos(\frac{2\pi t}{L}) + 0.1944\sin(\frac{2\pi t}{L}) \\ 1 - 0.02\sin(\frac{2\pi t}{L}) \end{bmatrix}$$

In implementation, at load pick-up, we verify that the distance between the quadrotor and load is consistently the cable length for 0.8 seconds before switching from the quadrotor controller to the quadrotor-with-load controller. This delay allows us to verify that the load was successfully picked up and avoids false switches during failed pick-up attempts. The load is released when the load reaches within a $5cm$ Euclidean distance of its desired release position and within $2cm/s$ of its desired release velocity in both directions.

Fig. 9 shows the results of this maneuver's execution, with the black vertical lines indicating switches between controllers. We see that the load angle and quadrotor attitude both reach angles of $20^o$. In addition, the load velocity reaches almost 2m/s.

The load is picked up around 15 seconds and released at around 23 seconds. At these points, the controller applied to the system switches. As seen in Figs. 9b, 9c, and 9g, the quadrotor states remain continuous through these transition points and, despite the switch in controller, state errors do not increase. Additionally, note the fast convergence of the load states in Figs. 9d - 9f to their desired drop conditions. However, as can be seen from the load path in Fig. 9a, the horizontal velocity at load release was not identically 0, resulting in some error in the final load position.

We also experiment with release of the load at a non-zero horizontal velocity. Here, we omit the load pick-up and simply focus on load release. The load trajectory parameters are: $(y_0, z_0) = (-1.2, 1.3), (y_1, z_1) = (1.2, 0), (y_r, z_r) = (0.8, 1.4), \dot{z}_r = 0.15, \phi_{L,r} = 20^o$, resulting in the desired load trajectory:

$$L = 3.3553$$
$$\mathbf{x}_L^d(t) = \begin{bmatrix} -0.2 - 1\cos(\frac{2\pi t}{L}) - 0.3885\sin(\frac{2\pi t}{L}) \\ 1.35 - 0.05\cos(\frac{2\pi t}{L}) - 0.0801\sin(\frac{2\pi t}{L}) \end{bmatrix}$$

Fig. 10 shows the load states at the release point, and we can clearly see that the load is in projectile motion. The resulting desired horizontal velocity at release was 0.73m/s. We can see the load reaches the ground at around 28 seconds, where it is close to its desired y-position of 1.2m.

## IX. Conclusion

We have analyzed the hybrid system of a quadrotor with a cable-suspended payload. Specifically, we derived a coordinate-free dynamic model of the system, proved the system's differential flatness properties, and designed controllers for its subsystems. Through this, we were able to cohesively apply methods traditionally used for non-hybrid systems work in this hybrid setting. Additionally, we proposed a trajectory generation method that, unlike previous works, considers the behavior of the full hybrid dynamics. We then applied these methods to designing an aggressive load-transport maneuver. Finally, we successfully demonstrated this maneuver with an Asctec Hummingbird quadrotor, which for the first time experimentally validates the proposed methods across the complete hybrid system.

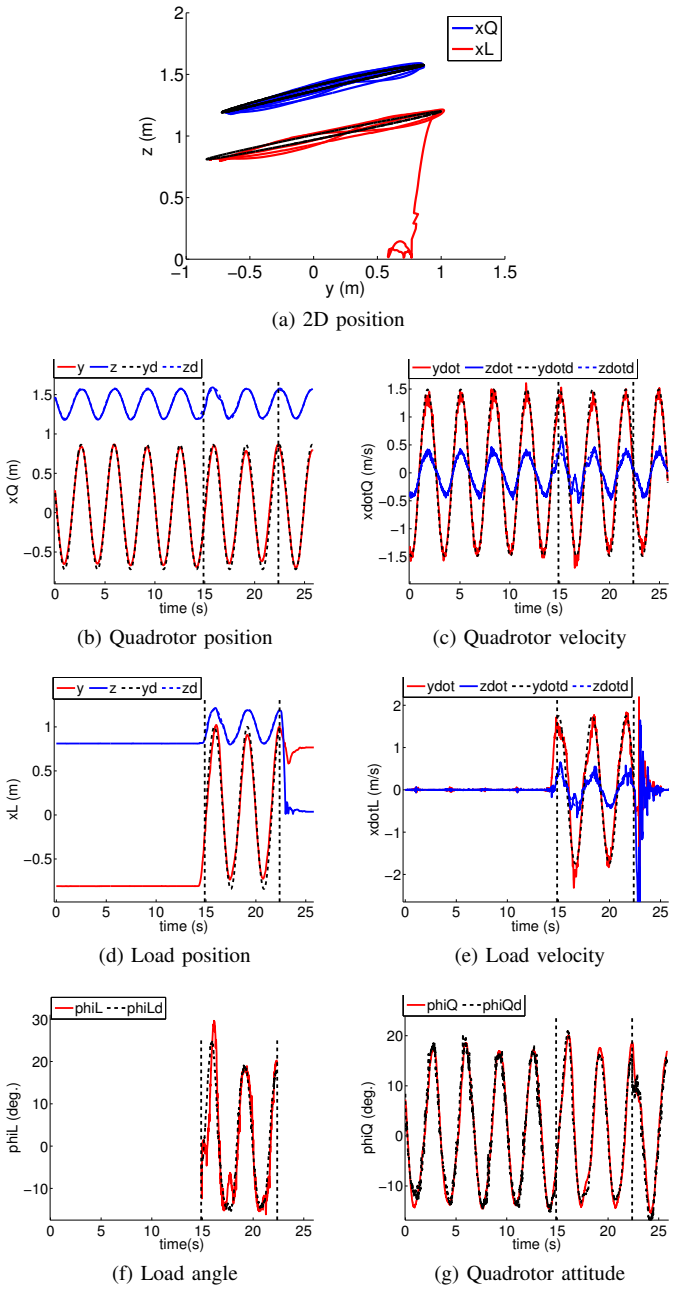


(a) 2D position

(b) Quadrotor position

(c) Quadrotor velocity

(d) Load position

(e) Load velocity

(f) Load angle

(g) Quadrotor attitude

Fig. 9: States over time, load-transport maneuver

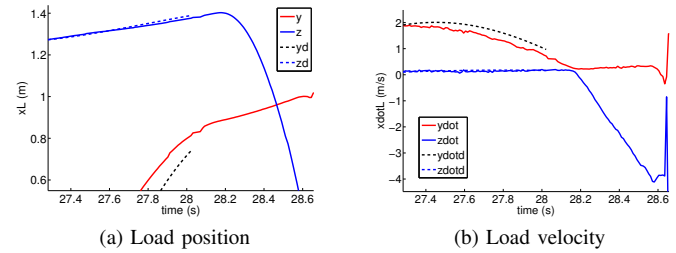


(a) Load position

(b) Load velocity

Fig. 10: Load states after release with initial vertical and horizontal velocity

## X. Future Work

There are a number of possible directions for future work. Firstly, we must extend these results for the planar system approximation to the full three-dimensional model. Further, we wish to eliminate the system's reliance on the VICON motion capture system. As a first step, we hope to derive the load state from a downward camera on the quadrotor before attempting a full vision-based approach. Additionally, we hope to examine the case of multiple quadrotors carrying a point-mass or rigid-body load and develop similar trajectory generation techniques for such a system.

## Acknowledgments

The author would like to thank Dr. Vijay Kumar and Dr. Koushil Sreenath for their guidance and support throughout this project. The author would also like to acknowledge Terry Kientz, for the design and construction of the quadrotor's electromagnet mechanism, and thank Justin Thomas and Kartik Mohta, all their assistance and patience while conducting experiments.

## APPENDIX A
## INTEGRATION OF ACTION INTEGRAL FOR QUADROTOR-WITH-LOAD SUBSYSTEM

Recall the action integral:

$$\begin{aligned}\delta S &= \int_{t_1}^{t_2} (\delta W + \delta \mathcal{L}) dt \\ &= \int_{t_1}^{t_2} (((m_Q + m_L)\dot{\mathbf{x}}_L - m_Q l\dot{\mathbf{p}}) \cdot \delta\dot{\mathbf{x}}_L \\ &\qquad +(fR\mathbf{e}_3 - (m_Q + m_L)g\mathbf{e}_3) \cdot \delta\mathbf{x}_L)\, dt \\ &\quad + \int_{t_1}^{t_2} \left((m_Q l^2\dot{\mathbf{p}} - m_Q l\dot{\mathbf{x}}_L) \cdot \delta\dot{\mathbf{p}}\right. \\ &\qquad \left. +(m_Q gl\mathbf{e}_3 - flR\mathbf{e}_3) \cdot \delta\mathbf{p}\right) dt \\ &\quad + \int_{t_1}^{t_2} \left(\Omega^T [\mathbb{I}]_{\mathcal{B}} \cdot \delta\Omega + M \cdot (R^T \delta R)\right) dt\end{aligned}$$

with variations:

$$\begin{aligned}\delta\mathbf{p} &= \xi \times \mathbf{p} \\ \delta R &= R\hat{\eta} \\ \delta\dot{\mathbf{p}} &= \dot{\xi} \times \mathbf{p} + \xi \times \dot{\mathbf{p}} \\ \delta\Omega &= \hat{\Omega}\eta + \dot{\eta}\end{aligned}$$

### A. Integrating the $\mathbf{x}_L$ term

Let:

$$\begin{aligned}u &= (m_Q + m_L)\dot{\mathbf{x}}_L - m_Q l\dot{\mathbf{p}} \\ du &= ((m_Q + m_L)\ddot{\mathbf{x}}_L - m_Q l\ddot{\mathbf{p}})dt \\ v &= \delta\mathbf{x}_L \\ dv &= \delta\dot{\mathbf{x}}_L dt\end{aligned}$$

Then:

$$\begin{aligned}&\int_{t_1}^{t_2} (((m_Q + m_L)\dot{\mathbf{x}}_L - m_Q l\dot{\mathbf{p}}) \cdot \delta\dot{\mathbf{x}}_L \\ &\qquad +(fR\mathbf{e}_3 - (m_Q + m_L)g\mathbf{e}_3) \cdot \delta\mathbf{x}_L)\, dt \\ &= (((m_Q + m_L)\dot{\mathbf{x}}_L - m_Q l\dot{\mathbf{p}}) \cdot \delta\mathbf{x}_L)\Big|_{t_1}^{t_2} \\ &\quad - \int_{t_1}^{t_2} (((m_Q + m_L)\ddot{\mathbf{x}}_L - m_Q l\ddot{\mathbf{p}}) \cdot \delta\mathbf{x}_L)\, dt \\ &\quad + \int_{t_1}^{t_2} ((fR\mathbf{e}_3 - (m_Q + m_L)g\mathbf{e}_3) \cdot \delta\mathbf{x}_L)\, dt \\ &= \int_{t_1}^{t_2} ((m_Q l\ddot{\mathbf{p}} - (m_Q + m_L)\ddot{\mathbf{x}}_L \\ &\qquad fR\mathbf{e}_3 - (m_Q + m_L)g\mathbf{e}_3) \cdot \delta\mathbf{x}_L)\, dt \qquad (108)\end{aligned}$$

### B. Integrating the $\mathbf{p}$ term

$$\begin{aligned}&\int_{t_1}^{t_2} \left((m_Q l^2\dot{\mathbf{p}} - m_Q l\dot{\mathbf{x}}_L) \cdot \delta\dot{\mathbf{p}}\right. \\ &\qquad \left. +(m_Q gl\mathbf{e}_3 - flR\mathbf{e}_3) \cdot \delta\mathbf{p}\right) dt \\ &= \int_{t_1}^{t_2} \Big((m_Q l^2\dot{\mathbf{p}} - m_Q l\dot{\mathbf{x}}_L) \cdot (\dot{\xi} \times \mathbf{p} + \xi \times \dot{\mathbf{p}}) \\ &\qquad +(m_Q gl\mathbf{e}_3 - flR\mathbf{e}_3) \cdot (\xi \times \mathbf{p})\Big)\, dt \\ &= \int_{t_1}^{t_2} \Big((\mathbf{p} \times (m_Q l^2\dot{\mathbf{p}} - m_Q l\dot{\mathbf{x}}_L)) \cdot \dot{\xi} \\ &+ \left(\dot{\mathbf{p}} \times (m_Q l^2\dot{\mathbf{p}} - m_Q l\dot{\mathbf{x}}_L) + \mathbf{p} \times (m_Q gl\mathbf{e}_3 - flR\mathbf{e}_3)\right) \cdot \xi\Big)\, dt\end{aligned}$$

Let:

$$\begin{aligned}u &= \mathbf{p} \times (m_Q l^2\dot{\mathbf{p}} - m_Q l\dot{\mathbf{x}}_L) \\ du &= (\dot{\mathbf{p}} \times (m_Q l^2\dot{\mathbf{p}} - m_Q l\dot{\mathbf{x}}_L)) + (\mathbf{p} \times (m_Q l^2\ddot{\mathbf{p}} - m_Q l\ddot{\mathbf{x}}_L))dt \\ v &= \xi \\ dv &= \dot{\xi}dt\end{aligned}$$

Then:

$$\begin{aligned}&\int_{t_1}^{t_2} \Big((\mathbf{p} \times (m_Q l^2\dot{\mathbf{p}} - m_Q l\dot{\mathbf{x}}_L)) \cdot \dot{\xi} \\ &+ \left(\dot{\mathbf{p}} \times (m_Q l^2\dot{\mathbf{p}} - m_Q l\dot{\mathbf{x}}_L) - \mathbf{p} \times (m_Q gl\mathbf{e}_3 + flR\mathbf{e}_3)\right) \cdot \xi\Big)\, dt \\ &= \left(\mathbf{p} \times (m_Q l^2\dot{\mathbf{p}} - m_Q l\dot{\mathbf{x}}_L) \cdot \xi\right)\Big|_{t_1}^{t_2} \\ &\quad - \int_{t_1}^{t_2} \left((\dot{\mathbf{p}} \times (m_Q l^2\dot{\mathbf{p}} - m_Q l\dot{\mathbf{x}}_L))\right. \\ &\qquad \left. +(\mathbf{p} \times (m_Q l^2\ddot{\mathbf{p}} - m_Q l\ddot{\mathbf{x}}_L)) \cdot \xi\right) dt \\ &\quad + \int_{t_1}^{t_2} \left((\dot{\mathbf{p}} \times (m_Q l^2\dot{\mathbf{p}} - m_Q l\dot{\mathbf{x}}_L)\right. \\ &\qquad \left. +\mathbf{p} \times (m_Q gl\mathbf{e}_3 - flR\mathbf{e}_3)) \cdot \xi\right) dt \\ &= \int_{t_1}^{t_2} \left((\mathbf{p} \times (m_Q gl\mathbf{e}_3 - flR\mathbf{e}_3 + m_Q l\ddot{\mathbf{x}}_L - m_Q l^2\ddot{\mathbf{p}})) \cdot \xi\right) dt \qquad (109)\end{aligned}$$

### C. Integrating the $R$ term

$$\begin{aligned}&\int_{t_1}^{t_2} \left([\mathbb{I}]_{\mathcal{B}}\Omega \cdot \delta\Omega + \mathbf{M}(R^T \delta R)\right) dt \\ &= \int_{t_1}^{t_2} ([\mathbb{I}]_{\mathcal{B}}\Omega \cdot (\Omega \times \eta + \dot{\eta}) + \mathbf{M}\hat{\eta})\, dt \\ &= \int_{t_1}^{t_2} (([\mathbb{I}]_{\mathcal{B}}\Omega \times \Omega) \cdot \eta + [\mathbb{I}]_{\mathcal{B}}\Omega \cdot \dot{\eta} + \mathbf{M} \cdot \eta)\, dt \\ &= \int_{t_1}^{t_2} \Big(([\mathbb{I}]_{\mathcal{B}}\Omega \times \Omega) \cdot \eta + \frac{d}{dt}([\mathbb{I}]_{\mathcal{B}}\Omega \cdot \eta) \\ &\qquad -[\mathbb{I}]_{\mathcal{B}}\dot{\Omega} \cdot \eta + \mathbf{M} \cdot \eta\Big)\, dt \\ &= \int_{t_1}^{t_2} \left((-\Omega \times [\mathbb{I}]_{\mathcal{B}}\Omega - [\mathbb{I}]_{\mathcal{B}}\dot{\Omega} + M) \cdot \eta\right) dt \qquad (110)\end{aligned}$$

### D. Simplification of equations of motion

Recall the equations from setting all variations to 0:

$$m_Q l\ddot{\mathbf{p}} - (m_Q + m_L)\ddot{\mathbf{x}}_L - (m_Q + m_L)g\mathbf{e}_3 + fR\mathbf{e}_3 = 0 \tag{111}$$

$$\mathbf{p} \times (m_Q gl\mathbf{e}_3 - flR\mathbf{e}_3 + m_Q l\ddot{\mathbf{x}}_L - m_Q l^2\ddot{\mathbf{p}}) = 0 \tag{112}$$

$$-\Omega \times [\mathbb{I}]_{\mathcal{B}}\Omega - [\mathbb{I}]_{\mathcal{B}}\dot{\Omega} + M = 0 \tag{113}$$

Taking the cross product of $\mathbf{p}$ and Eq. 111:

$$\mathbf{p} \times (m_Q l\ddot{\mathbf{p}} - (m_Q + m_L)\ddot{\mathbf{x}}_L - (m_Q + m_L)g\mathbf{e}_3 + fR\mathbf{e}_3) = 0$$

Adding this to Eq. 112 gives:

$$-m_L\mathbf{p} \times \ddot{\mathbf{x}}_L - m_L g\mathbf{p} \times \mathbf{e}_3 = 0 \tag{114}$$

$$\mathbf{p} \times \ddot{\mathbf{x}}_L = -g\mathbf{p} \times \mathbf{e}_3 \tag{115}$$

In addition, differentiating the definition $\dot{\mathbf{p}} = \omega \times \mathbf{p}$ gives:

$$\ddot{\mathbf{p}} = \dot{\omega} \times \mathbf{p} + \omega \times \dot{\mathbf{p}} = 0, \tag{116}$$

and the last term of Eq. 112 can be rewritten as:

$$\begin{aligned}\mathbf{p} \times \ddot{\mathbf{p}} &= \mathbf{p} \times (\dot{\omega} \times \mathbf{p} + \omega \times \dot{\mathbf{p}}) \\ &= \dot{\omega}(\mathbf{p} \cdot \mathbf{p}) - \mathbf{p}(\mathbf{p} \cdot \dot{\omega}) + \omega(\mathbf{p} \cdot \dot{\mathbf{p}}) - \dot{\mathbf{p}}(\mathbf{p} \cdot \omega) \\ &= \dot{\omega}\end{aligned} \tag{117}$$

Substituting Eqs. 115 and 117 into Eq. 112 gives:

$$\begin{aligned}\mathbf{p} \times (m_Q g\mathbf{e}_3 - fR\mathbf{e}_3) - m_Q g\mathbf{p} \times \mathbf{e}_3 - m_Q l\dot{\omega} = 0 \\ m_Q l\dot{\omega} = -fR\mathbf{p} \times \mathbf{e}_3\end{aligned} \tag{118}$$

Now, note the identity:

$$\begin{aligned}\frac{d}{dt}(\mathbf{p} \cdot \dot{\mathbf{p}}) &= \mathbf{p} \cdot \ddot{\mathbf{p}} + \dot{\mathbf{p}} \cdot \dot{\mathbf{p}} = 0 \\ \mathbf{p} \times (\mathbf{p} \times \ddot{\mathbf{p}}) &= \mathbf{p}(\mathbf{p} \cdot \ddot{\mathbf{p}}) - \ddot{\mathbf{p}}(\mathbf{p} \cdot \mathbf{p}) \\ &= -(\dot{\mathbf{p}} \cdot \dot{\mathbf{p}})\mathbf{p} - \ddot{\mathbf{p}} \\ \ddot{\mathbf{p}} &= -(\dot{\mathbf{p}} \cdot \dot{\mathbf{p}})\mathbf{p} - \mathbf{p} \times (\mathbf{p} \times \ddot{\mathbf{p}})\end{aligned}$$

Eq. 111 becomes:

$$\begin{aligned}-m_Q l(\dot{\mathbf{p}} \cdot \dot{\mathbf{p}})\mathbf{p} - m_Q l(\mathbf{p} \times (\mathbf{p} \times \ddot{\mathbf{p}})) \\ -(m_Q + m_L)(\ddot{\mathbf{x}}_L + g\mathbf{e}_3) + fR\mathbf{e}_3 = 0\end{aligned} \tag{119}$$

From Eq. 112, we can solve for:

$$\mathbf{p} \times \ddot{\mathbf{p}} = \frac{1}{m_Q l}\left(\mathbf{p} \times (m_Q g\mathbf{e}_3 - fR\mathbf{e}_3 + m_Q\ddot{\mathbf{x}}_L)\right)$$

Substituting this into Eq. 119:

$$\begin{aligned}&-m_Q l(\dot{\mathbf{p}} \cdot \dot{\mathbf{p}})\mathbf{p} - \mathbf{p} \times (\mathbf{p} \times (m_Q g\mathbf{e}_3 - fR\mathbf{e}_3 + m_Q\ddot{\mathbf{x}}_L)) \\ &\quad -(m_Q + m_L)(\ddot{\mathbf{x}}_L + g\mathbf{e}_3) + fR\mathbf{e}_3 \\ &= -m_Q l(\dot{\mathbf{p}} \cdot \dot{\mathbf{p}})\mathbf{p} + \mathbf{p}(\mathbf{p} \cdot fR\mathbf{e}_3) - fR\mathbf{e}_3 \cdot (\mathbf{p} \cdot \mathbf{p}) \\ &\quad -m_Q\mathbf{p} \times (\mathbf{p} \times (g\mathbf{e}_3 + \ddot{\mathbf{x}}_L)) \\ &\quad -(m_Q + m_L)(\ddot{\mathbf{x}}_L + g\mathbf{e}_3) + fR\mathbf{e}_3\end{aligned}$$

From Eq. 114, $\mathbf{p} \times (\ddot{\mathbf{x}}_L + g\mathbf{e}_3) = 0$ and we further simplify:

$$\begin{aligned}(-m_Q l(\dot{\mathbf{p}} \cdot \dot{\mathbf{p}}) + \mathbf{p} \cdot fR\mathbf{e}_3)\mathbf{p} - (m_Q + m_L)(\ddot{\mathbf{x}}_L + g\mathbf{e}_3) = 0 \\ (m_Q + m_L)(\ddot{\mathbf{x}}_L + g\mathbf{e}_3) = (\mathbf{p} \cdot fR\mathbf{e}_3 - m_Q l(\dot{\mathbf{p}} \cdot \dot{\mathbf{p}}))\mathbf{p}\end{aligned} \tag{120}$$

Eqs. 113, 118, and 120 are the equations of motion.

## APPENDIX B
## DIFFERENTIAL FLATNESS OF QUADROTOR-WITH-LOAD SUBSYSTEM

Recall the states:

$$\mathbf{x}_1 = [\mathbf{x}_L \;\; \dot{\mathbf{x}}_L \;\; \mathbf{p} \;\; \omega \;\; {}^{\mathcal{I}}R_{\mathcal{B}} \;\; {}^{\mathcal{I}}\Omega_{\mathcal{B}}^{\mathcal{B}}]^T,$$

input:

$$\mathbf{u} = [f \;\; \mathbf{M}]^T,$$

and proposed flat outputs:

$$\mathbf{y}_1 = [\mathbf{x}_L \;\; \psi]^T$$

We have already determined the states:

$$\begin{aligned}T &= m_L\|g\mathbf{e}_3 + \ddot{\mathbf{x}}_L\| \\ \mathbf{p} &= \frac{-(\ddot{\mathbf{x}}_L + g\mathbf{e}_3)}{\|\ddot{\mathbf{x}}_L + g\mathbf{e}_3\|} \\ \dot{T} &= -m_L(\dddot{\mathbf{x}}_L \cdot \mathbf{p}) \\ \dot{\mathbf{p}} &= \frac{-(m_L\dddot{\mathbf{x}}_L + \dot{T}\mathbf{p})}{T} \\ \omega &= \frac{m_L}{T}\dddot{\mathbf{x}}_L \times \mathbf{p} \\ \mathbf{x}_Q &= \mathbf{x}_L - l\mathbf{p}\end{aligned}$$

Further, the equation of motion and its first derivative are:

$$\begin{aligned}-T\mathbf{p} - m_L g\mathbf{e}_3 &= m_L\ddot{\mathbf{x}}_L \\ -T\dot{\mathbf{p}} - \dot{T}\mathbf{p} &= m_L\dddot{\mathbf{x}}_L\end{aligned}$$

We can differentiate $\dot{T}$ to obtain:

$$\ddot{T} = -m_L(\mathbf{x}_L^{(4)} \cdot \mathbf{p} + \ddot{\mathbf{x}}_L \cdot \dot{\mathbf{p}})$$

Then, differentiating the equation of motion again:

$$\begin{aligned}-T\ddot{\mathbf{p}} - 2\dot{T}\dot{\mathbf{p}} - \ddot{T}\mathbf{p} &= m_L\mathbf{x}_L^{(4)} \\ \ddot{\mathbf{p}} &= \frac{-(m_L\mathbf{x}_L^{(4)} + 2\dot{T}\dot{\mathbf{p}} + \ddot{T}\mathbf{p})}{T} \\ \dot{\omega} &= m_L(\mathbf{x}_L^{(4)} \times \mathbf{p} + \ddot{\mathbf{x}}_L \times \dot{\mathbf{p}})\end{aligned}$$

Repeating this process twice more, we see:

$$\begin{aligned}\dddot{T} &= -m_L(\mathbf{x}_L^{(5)} \cdot \mathbf{p} + 2\mathbf{x}_L^{(4)} \cdot \dot{\mathbf{p}} + \dddot{\mathbf{x}}_L \cdot \ddot{\mathbf{p}}) \\ -T\dddot{\mathbf{p}} - 3\ddot{T}\dot{\mathbf{p}} - 3\dot{T}\ddot{\mathbf{p}} - \dddot{T}\mathbf{p} &= m_L\mathbf{x}_L^{(5)} \\ \dddot{\mathbf{p}} &= \frac{-(m_L\mathbf{x}_L^{(5)} + 3\ddot{T}\dot{\mathbf{p}} + 3\dot{T}\ddot{\mathbf{p}} + \dddot{T}\mathbf{p})}{T} \\ \ddot{\omega} &= m_L(\mathbf{x}_L^{(5)} \times \mathbf{p} + 2\mathbf{x}_L^{(4)} \times \dot{\mathbf{p}} + \dddot{\mathbf{x}}_L \times \ddot{\mathbf{p}})\end{aligned}$$

and:

$$\begin{aligned}T^{(4)} &= -m_L(\mathbf{x}_L^{(6)} \cdot \mathbf{p} + 3\mathbf{x}_L^{(5)} \cdot \dot{\mathbf{p}} + 3\mathbf{x}_L^{(4)} \cdot \ddot{\mathbf{p}} + \dddot{\mathbf{x}}_L \cdot \dddot{\mathbf{p}}) \\ -T\mathbf{p}^{(4)} - 4\dddot{T}\dot{\mathbf{p}} - 6\ddot{T}\ddot{\mathbf{p}} - 4\dot{T}\dddot{\mathbf{p}} - T^{(4)}\mathbf{p} &= m_L\mathbf{x}_L^{(6)} \\ \mathbf{p}^{(4)} &= \frac{-(m_L\mathbf{x}_L^{(6)} + 4\dddot{T}\dot{\mathbf{p}} + 6\ddot{T}\ddot{\mathbf{p}} + 4\dot{T}\dddot{\mathbf{p}} + T^{(4)}\mathbf{p})}{T} \\ \ddot{\omega} &= m_L(\mathbf{x}_L^{(6)} \times \mathbf{p} + 3\mathbf{x}_L^{(5)} \times \dot{\mathbf{p}} + 3\mathbf{x}_L^{(4)} \times \ddot{\mathbf{p}} + \dddot{\mathbf{x}}_L \times \dddot{\mathbf{p}})\end{aligned}$$

This allows us to find the quadrotor states:

$$\begin{aligned}\dot{\mathbf{x}}_Q &= \dot{\mathbf{x}}_L - l\dot{\mathbf{p}}\\ \ddot{\mathbf{x}}_Q &= \ddot{\mathbf{x}}_L - l\ddot{\mathbf{p}}\\ \dddot{\mathbf{x}}_Q &= \dddot{\mathbf{x}}_L - l\dddot{\mathbf{p}}\\ \mathbf{x}_Q^{(4)} &= \mathbf{x}_L^{(4)} - l\mathbf{p}^{(4)}\end{aligned}$$

Now, we can find the states $R$ and $\Omega$ and the inputs $f$ and $\mathbf{M}$ as:

$$\begin{aligned}fR\mathbf{e}_3 &= -m_Q l\ddot{\mathbf{p}} + (m_Q + m_L)(\ddot{\mathbf{x}}_L + g\mathbf{e}_3)\\ &= m_L(\ddot{\mathbf{x}}_L + g\mathbf{e}_3) + m_Q(\ddot{\mathbf{x}}_Q + g\mathbf{e}_3)\\ \mathbf{b}_3 &= \frac{m_L(\ddot{\mathbf{x}}_L + g\mathbf{e}_3) + m_Q(\ddot{\mathbf{x}}_Q + g\mathbf{e}_3)}{\|m_L(\ddot{\mathbf{x}}_L + g\mathbf{e}_3) + m_Q(\ddot{\mathbf{x}}_Q + g\mathbf{e}_3)\|}\\ f &= \|m_L(\ddot{\mathbf{x}}_L + g\mathbf{e}_3) + m_Q(\ddot{\mathbf{x}}_Q + g\mathbf{e}_3)\|\end{aligned}$$

With this value of $\mathbf{b}_3$ and $\psi$ from the flat outputs, we can find $R$ as done for the quadrotor subsystem.

Next, we differentiate the equation of motion and find:

$$\begin{aligned}\dot{f}\mathbf{b}_3 + f({}^{\mathcal{I}}\Omega^{\mathcal{B}} \times \mathbf{b}_3) &= m_Q\dddot{\mathbf{x}}_Q + m_L\dddot{\mathbf{x}}_L\\ \dot{f} &= (m_Q\dddot{\mathbf{x}}_Q + m_L\dddot{\mathbf{x}}_L)\cdot\mathbf{b}_3\end{aligned}$$

We can use this value of $\dot{f}$ and Eqs. 57 - 61 to solve for ${}^{\mathcal{I}}\Omega^{\mathcal{B}}_{\mathcal{B}}$.

Differentiating the equation of motion again:

$$\begin{aligned}&\ddot{f}\mathbf{b}_3 + 2\dot{f}\left({}^{\mathcal{I}}\Omega^{\mathcal{B}} \times \mathbf{b}_3\right) + f\left({}^{\mathcal{I}}\alpha^{\mathcal{B}} \times \mathbf{b}_3 + {}^{\mathcal{I}}\Omega^{\mathcal{B}} \times ({}^{\mathcal{I}}\Omega^{\mathcal{B}} \times \mathbf{b}_3)\right)\\ &\quad = (m_Q\mathbf{x}_Q^{(4)} + m_L\mathbf{x}_L^{(4)})\\ &\ddot{f} = (m_Q\mathbf{x}_Q^{(4)} + m_L\mathbf{x}_L^{(4)})\cdot\mathbf{b}_3\\ &\quad - 2\dot{f}\left({}^{\mathcal{I}}\Omega^{\mathcal{B}} \times \mathbf{b}_3\right) - f{}^{\mathcal{I}}\Omega^{\mathcal{B}} \times ({}^{\mathcal{I}}\Omega^{\mathcal{B}} \times \mathbf{b}_3)\end{aligned}$$

With $\ddot{f}$, Sec. IV-A describes finding of components of ${}^{\mathcal{I}}\dot{\Omega}^{\mathcal{B}}_{\mathcal{B}}$.

Finally, we find the moment with:

$$\mathbf{M} = {}^{\mathcal{I}}\Omega^{\mathcal{B}}_{\mathcal{B}} \times [\mathbb{I}]_{\mathcal{B}}{}^{\mathcal{I}}\Omega^{\mathcal{B}}_{\mathcal{B}} + [\mathbb{I}]_{\mathcal{B}}{}^{\mathcal{I}}\dot{\Omega}^{\mathcal{B}}_{\mathcal{B}}$$

Note that here, ${}^{\mathcal{I}}\dot{\Omega}^{\mathcal{B}}_{\mathcal{B}}$ is a function of $\ddot{f}$, which is in turn a function of $\mathbf{x}_Q^{(4)}$. $\mathbf{x}_Q^{(4)}$ is derived from $\mathbf{p}^{(4)}$, which is a function of the sixth derivative of $\mathbf{x}_L$.

## APPENDIX C
## PROOF OF STABILITY OF QUADROTOR SUBSYSTEM CONTROLLER

### A. Exponential stability of position controller for $|e_Q(0)| < \frac{\pi}{2}$

Recall Eqs. 86 and 87, which prove the existence of a Lyapunov function for the attitude dynamics, $V_Q$, that satisfies:

$$\mathbf{z}_Q^T M_q \mathbf{z}_Q \leq V_Q \leq \mathbf{z}_Q^T M_Q \mathbf{z}_Q \tag{121}$$

$$\dot{V}_Q \leq -\mathbf{z}_Q^T W_Q \mathbf{z}_Q \tag{122}$$

Next, recall the definitions of the position controller, given in Eqs. 82 - 85:

$$\begin{aligned}&\mathbf{e}_x = \mathbf{x}_Q - \mathbf{x}_Q^d, \dot{\mathbf{e}}_x = \dot{\mathbf{x}}_Q - \dot{\mathbf{x}}_Q^d\\ &\mathbf{F}^d = -K_p\mathbf{e}_x - K_d\dot{\mathbf{e}}_x + m_Q(g\mathbf{e}_3 + \ddot{\mathbf{x}}_Q^d)\\ &f^d = \mathbf{F}^d\cdot\mathbf{b}_3\\ &\mathbf{b}_3^d = \frac{\mathbf{F}^d}{\|\mathbf{F}^d\|},\end{aligned}$$

and the bounds:

$$\begin{aligned}|e_Q(0)| &< \frac{\pi}{2}\\ \|\mathbf{e}_x(0)\| &< \mathbf{e}_{x,max}\\ \|m_Q(g\mathbf{e}_3 + \ddot{\mathbf{x}}_Q^d)\| &\leq Y\end{aligned}$$

Consider a constant $c > 0$ and the function:

$$V_x = \frac{1}{2}K_p\mathbf{e}_x\cdot\mathbf{e}_x + \frac{1}{2}m_Q\dot{\mathbf{e}}_x\cdot\dot{\mathbf{e}}_x + c\mathbf{e}_x\cdot\dot{\mathbf{e}}_x \tag{123}$$

Define $\mathbf{z}_x = [\|\mathbf{e}_x\| \;\; \|\dot{\mathbf{e}}_x\|]^T$. Eq. 123 satisfies:

$$\mathbf{z}_x^T M_x \mathbf{z}_x \leq V_x \leq \mathbf{z}_x^T M_X \mathbf{z}_x, \tag{124}$$

where:

$$\begin{aligned}M_x &= \begin{bmatrix}\frac{K_p}{2} & -\frac{c}{2}\\ -\frac{c}{2} & \frac{m_Q}{2}\end{bmatrix}\\ M_X &= \begin{bmatrix}\frac{K_p}{2} & \frac{c}{2}\\ \frac{c}{2} & \frac{m_Q}{2}\end{bmatrix}\end{aligned}$$

Assume $K_p > 0$, $K_d > 0$. To ensure that $M_x$ and $M_X$ are positive definite, we need:

$$\begin{aligned}\det M_x = \det M_X &= \frac{m_Q K_p}{4} - \frac{c^2}{4} > 0\\ c &< \sqrt{m_Q K_p}\end{aligned} \tag{125}$$

Next, take the derivative of Eq. 123:

$$\dot{V}_x = K_p\mathbf{e}_x\cdot\dot{\mathbf{e}}_x + c\dot{\mathbf{e}}_x\cdot\dot{\mathbf{e}}_x + \ddot{\mathbf{e}}_x\cdot(m_Q\dot{\mathbf{e}}_x + c\mathbf{e}_x) \tag{126}$$

Using the equation of motion, the error dynamics are:

$$\begin{aligned}m_Q\ddot{\mathbf{e}}_x &= m_Q(\ddot{\mathbf{x}}_Q - \ddot{\mathbf{x}}_Q^d)\\ &= -m_Q g\mathbf{e}_3 + f^d\mathbf{b}_3 - m_Q\ddot{\mathbf{x}}_Q^d\\ &= -m_Q g\mathbf{e}_3 - m_Q\ddot{\mathbf{x}}_Q^d + \mathbf{F}^d + f^d\mathbf{b}_3 - \mathbf{F}^d\end{aligned} \tag{127}$$

Substituting in the designated $\mathbf{F}$ from the control law:

$$\begin{aligned}m_Q\ddot{\mathbf{e}}_x &= -m_Q g\mathbf{e}_3 - m_Q\ddot{\mathbf{x}}_Q^d - K_p\mathbf{e}_x - K_d\dot{\mathbf{e}}_x\\ &\quad + m_Q(g\mathbf{e}_3 + \ddot{\mathbf{x}}_Q^d) + X\\ &= -K_p\mathbf{e}_x - K_d\dot{\mathbf{e}}_x + X,\end{aligned} \tag{128}$$

where:

$$\begin{aligned} X &= f^d\mathbf{b}_3 - \mathbf{F}^d \\ &= (\mathbf{F}^d \cdot \mathbf{b}_3)\mathbf{b}_3 - \|\mathbf{F}^d\|\mathbf{b}_3^d \\ &= \|\mathbf{F}^d\|((\mathbf{b}_3^d \cdot \mathbf{b}_3)\mathbf{b}_3 - \mathbf{b}_3^d) \end{aligned}$$

Substituting the definition of $\ddot{\mathbf{e}}_x$ from Eq. 128 into Eq. 126:

$$\begin{aligned} \dot{V}_x &= K_p\mathbf{e}_x \cdot \dot{\mathbf{e}}_x + c\dot{\mathbf{e}}_x \cdot \dot{\mathbf{e}}_x \\ &\quad + (-\frac{K_p}{m_Q}\mathbf{e}_x - \frac{K_d}{m_Q}\dot{\mathbf{e}}_x + \frac{X}{m_Q}) \cdot (m_Q\dot{\mathbf{e}}_x + c\mathbf{e}_x) \\ &= -(K_d - c)\dot{\mathbf{e}}_x \cdot \dot{\mathbf{e}}_x - \frac{cK_p}{m_Q}\mathbf{e}_x \cdot \mathbf{e}_x \\ &\quad - \frac{cK_d}{m_Q}\mathbf{e}_x \cdot \dot{\mathbf{e}}_x + X \cdot (\dot{\mathbf{e}}_x + \frac{c}{m_Q}\mathbf{e}_x) \end{aligned}$$

Applying the Cauchy-Schwartz Inequality, $|\mathbf{a}\cdot\mathbf{b}| \leq \|\mathbf{a}\|\|\mathbf{b}\|$:

$$\begin{aligned} \dot{V}_x \leq &-(K_d - c)\|\dot{\mathbf{e}}_x\|^2 - \frac{cK_p}{m_Q}\|\mathbf{e}_x\|^2 - \frac{cK_d}{m_Q}\|\mathbf{e}_x\|\|\dot{\mathbf{e}}_x\| \\ &+ \|X\|(\|\dot{\mathbf{e}}_x\| + \frac{c}{m_Q}\|\mathbf{e}_x\|) \end{aligned} \tag{129}$$

From the definition of $X$:

$$\begin{aligned} \|X\| &\leq \|\mathbf{F}^d\|\|(\mathbf{b}_3 \cdot \mathbf{b}_3^d)\mathbf{b}_3 - \mathbf{b}_3^d\| \\ &= \| - K_p\mathbf{e}_x - K_d\dot{\mathbf{e}}_x + m_Q(g\mathbf{e}_3 + \ddot{\mathbf{x}}_Q^d)\| \\ &\qquad \|(\mathbf{b}_3 \cdot \mathbf{b}_3^d)\mathbf{b}_3 - \mathbf{b}_3^d\| \\ &\leq (K_p\|\mathbf{e}_x\| + K_d\|\dot{\mathbf{e}}_x\| + \|m_Q(g\mathbf{e}_3 + \ddot{\mathbf{x}}_Q^d)\|) \\ &\qquad \|(\mathbf{b}_3 \cdot \mathbf{b}_3^d)\mathbf{b}_3 - \mathbf{b}_3^d\| \end{aligned} \tag{130}$$

Note that:

$$\begin{aligned} \|(\mathbf{b}_3 \cdot \mathbf{b}_3^d)\mathbf{b}_3 - \mathbf{b}_3^d\| &= \|\mathbf{b}_3 \times (\mathbf{b}_3 \times \mathbf{b}_3^d)\| \\ &= \|\mathbf{b}_3\|\|\mathbf{b}_3 \times \mathbf{b}_3^d\|\sin(\theta_e) \\ &= \|\mathbf{b}_3\|\|\mathbf{b}_3\|\|\mathbf{b}_3^d\|\sin(|\phi_Q - \phi_Q^d|)\sin(\theta_e) \end{aligned}$$

$\theta_e$ is the angle between $\mathbf{b}_3$ and $\mathbf{b}_3 \times \mathbf{b}_3^d$. Since $\mathbf{b}_3 \times \mathbf{b}_3^d$ will be orthogonal to $\mathbf{b}_3$, $\sin(\theta_e) = 1$. We see then that:

$$\|(\mathbf{b}_3 \cdot \mathbf{b}_3^d)\mathbf{b}_3 - \mathbf{b}_3^d\| = \sin(|e_Q|)$$

We assume $\|m_Q(g\mathbf{e}_3 + \ddot{\mathbf{x}}_Q^d)\| \leq Y$. This allows us to simplify Eq. 130:

$$\|X\| \leq (K_p\|\mathbf{e}_x\| + K_d\|\dot{\mathbf{e}}_x\| + Y)\sin(|e_Q|) \tag{131}$$

Substituting this into Eq. 129 gives:

$$\begin{aligned} \dot{V}_x \leq &-(K_d - c)\|\dot{\mathbf{e}}_x\|^2 - \frac{cK_p}{m_Q}\|\mathbf{e}_x\|^2 - \frac{cK_d}{m_Q}\|\mathbf{e}_x\|\|\dot{\mathbf{e}}_x\| \\ &+ (K_p\|\mathbf{e}_x\| + K_d\|\dot{\mathbf{e}}_x\| + Y)\sin(|e_Q|)(\|\dot{\mathbf{e}}_x\| + \frac{c}{m_Q}\|\mathbf{e}_x\|) \end{aligned} \tag{132}$$

Since we already know that the attitude dynamics are exponentially stable, we know that $e_Q$ will always be decreasing. We have assumed that $|e_Q(0)| < \frac{\pi}{2}$. Thus, $\sin(|e_Q|) \leq \sin(|e_Q(0)|) \equiv \alpha < 1$. We also assume $\|\mathbf{e}_x\| < \mathbf{e}_{x,max}$. Using this in Eq. 133:

$$\begin{aligned} \dot{V}_x \leq &-(K_d(1-\alpha) - c)\|\dot{\mathbf{e}}_x\|^2 - \frac{cK_p}{m_Q}(1-\alpha)\|\mathbf{e}_x\|^2 \\ &- \frac{cK_d}{m}(1-\alpha)\|\mathbf{e}_x\|\|\dot{\mathbf{e}}_x\| + K_p\mathbf{e}_{x,max}\sin(|e_Q|)\|\dot{\mathbf{e}}_x\| \\ &+ Y\sin(|e_Q|)(\|\dot{\mathbf{e}}_x\| + \frac{c}{m_Q}\|\mathbf{e}_x\|) \end{aligned}$$

Using the trigonometric property: $|\sin(\theta)| \leq |\theta|$, we can further simplify:

$$\begin{aligned} \dot{V}_x \leq &-(K_d(1-\alpha) - c)\|\dot{\mathbf{e}}_x\|^2 - \frac{cK_p}{m_Q}(1-\alpha)\|\mathbf{e}_x\|^2 \\ &- \frac{cK_d}{m}(1-\alpha)\|\mathbf{e}_x\|\|\dot{\mathbf{e}}_x\| + K_p\mathbf{e}_{x,max}|e_Q|\|\dot{\mathbf{e}}_x\| \\ &+ Y|e_Q|(\|\dot{\mathbf{e}}_x\| + \frac{c}{m_Q}\|\mathbf{e}_x\|) \end{aligned}$$

Define $\mathbf{z}_x$ and $\mathbf{z}_Q$ as before. Then:

$$\dot{V}_x \leq -\mathbf{z}_x^T W_x \mathbf{z}_x + \mathbf{z}_x^T W_{xQ}\mathbf{z}_Q, \tag{133}$$

where, as stated in Eqs. 88 and 89 :

$$W_{xQ} = \begin{bmatrix} \frac{cY}{m_Q} & 0 \\ Y + K_p\mathbf{e}_{x,max} & 0 \end{bmatrix}$$

$$W_x = \begin{bmatrix} \frac{cK_p}{m_Q}(1-\alpha) & \frac{1}{2}\frac{cK_d}{m_Q}(1-\alpha) \\ \frac{1}{2}\frac{cK_d}{m_Q}(1-\alpha) & K_d(1-\alpha) - c \end{bmatrix}$$

To ensure that $W_x$ is positive-definite for positive $\alpha, K_p$, and $K_d$, we require:

$$\frac{cK_p}{m_Q}(1-\alpha) > 0,\ c > 0 \tag{134}$$

$$K_d(1-\alpha) - c > 0,\ c < K_d(1-\alpha) \tag{135}$$

and:

$$\begin{aligned} \det W_{xQ} &= \frac{cK_p}{m_Q}(1-\alpha)(K_d(1-\alpha) - c) - \frac{1}{4}(\frac{cK_d}{m_Q}(1-\alpha))^2 \\ &= c\left(\frac{K_pK_d}{m_Q}(1-\alpha)^2 \right. \\ &\quad \left. -c\left(\frac{K_p}{m_Q}(1-\alpha) + \frac{K_d^2}{4m_Q^2}(1-\alpha)^2\right)\right) > 0 \end{aligned}$$

$$c < \frac{4m_QK_pK_d(1-\alpha)}{4m_QK_p + K_d^2(1-\alpha)} \tag{136}$$

Finally, consider the Lyapunov function:

$$V = V_Q + V_x \tag{137}$$

Using Eqs. 121 and 124, we see that:

$$\mathbf{z}_Q^T M_q \mathbf{z}_Q + \mathbf{z}_x^T M_x \mathbf{z}_x \leq V \leq \mathbf{z}_q^T M_Q \mathbf{z}_q + \mathbf{z}_x^T M_X \mathbf{z}_x,$$

and $V$ is positive-definite.

Differentiating the proposed Lyapunov function gives:

$$\dot{V} = \dot{V}_Q + \dot{V}_x \tag{138}$$

Using Eqs. 122 and 133, we see that:

$$\dot{V} \leq -\mathbf{z}_Q^T W_Q \mathbf{z}_Q + \mathbf{z}_x^T W_{xQ}\mathbf{z}_Q - \mathbf{z}_x^T W_x \mathbf{z}_x$$

Conditions in Eqs. 125, 135, and 136 tell us that for positive $c, \alpha, K_p, K_d$, the matrices $M_x, M_X, W_x$ will be positive-definite if:

$$c < \min\left\{\sqrt{m_Q K_p}, K_d(1-\alpha), \frac{4m_Q K_p K_d(1-\alpha)}{4m_Q K_p + K_d^2(1-\alpha)}\right\}$$

Further:

$$\begin{aligned}\dot{V} \leq &-\lambda_m(W_Q)\|\mathbf{z}_Q\|^2 + \|W_{xQ}\|_2\|\mathbf{z}_x\|\|\mathbf{z}_Q\| \\ &- \lambda_m(W_x)\|\mathbf{z}_x\|^2\end{aligned}$$

Here, $\lambda_m(\cdot)$ denotes the minimum eigenvalue of the matrix. Since $W_Q$ and $W_X$ are positive-definite, their minimum eigenvalues are positive non-zero. To ensure that $\dot{V}$ is negative-definite, we need:

$$\begin{aligned}-\dot{V} &\geq \lambda_m(W_Q)\|\mathbf{z}_Q\|^2 - \|W_{xQ}\|_2\|\mathbf{z}_x\|\|\mathbf{z}_Q\| + \lambda_m(W_x)\|\mathbf{z}_x\|^2 \\ &= \frac{1}{4\lambda_m(W_Q)}\left(4\lambda_m^2(W_Q)\|\mathbf{z}_Q\|^2\right. \\ &\quad \left. -4\lambda_m(W_Q)\|W_{xQ}\|_2\|\mathbf{z}_x\|\|\mathbf{z}_Q\| + \|W_{xQ}\|^2\|\mathbf{z}_x\|^2\right) \\ &\quad + \lambda_m(W_x)\|\mathbf{z}_x\|^2 - \frac{\|W_{xQ}\|^2\|\mathbf{z}_x\|^2}{4\lambda_m(W_Q)} \\ &= \frac{(2\lambda_m(W_Q)\|\mathbf{z}_Q\| - \|W_{xQ}\|\|\mathbf{z}_x\|)^2}{4\lambda_m(W_Q)} \\ &\quad + \left(\lambda_m(W_x)\|\mathbf{z}_x\|^2 - \frac{\|W_{xQ}\|^2\|\mathbf{z}_x\|^2}{4\lambda_m(W_Q)}\right) > 0\end{aligned}$$

The first quadratic term will always be positive. Thus, we only need:

$$\begin{aligned}&\left(\lambda_m(W_x)\|\mathbf{z}_x\|^2 - \frac{\|W_{xQ}\|^2\|\mathbf{z}_x\|^2}{4\lambda_m(W_Q)}\right) > 0 \\ &\lambda_m(W_x) > \frac{\|W_{xQ}\|^2}{4\lambda_m(W_Q)}\end{aligned}$$

These are the conditions given in Eqs. 90 and 91. If these are met, the origin of the error states $[e_Q \quad \dot{e}_Q \quad \mathbf{e}_x \quad \dot{\mathbf{e}}_x]^T$ is exponentially stable. Note that the position error $\mathbf{e}_{x,max}$ can be arbitrarily large, as long as conditions on $c, K_p, K_d$ can still be met.

### *B. Exponential attractiveness of position controller for $|e_Q(0)| \geq \frac{\pi}{2}$*

Next, we wish to show that when $|e_Q(0)| \geq \frac{\pi}{2}$, the origin of the error states $[e_Q \quad \dot{e}_Q \quad \mathbf{e}_x \quad \dot{\mathbf{e}}_x]^T$ is exponentially attractive. We know that the attitude dynamics are exponentially stable, so for any initial condition, there exists a time $t^*$ after which $|e_Q| < \frac{\pi}{2}$ and the full error dynamics become exponentially stable. We need to further guarantee that the error state $\mathbf{z}_x = [\mathbf{e}_x \quad \dot{\mathbf{e}}_x]^T$ remains bounded in $[0, t^*]$.

Consider the Lyapunov function:

$$V_{x_2} = \frac{1}{2}\|\mathbf{e}_x\|^2 + \frac{m_Q}{2}\|\dot{\mathbf{e}}_x\|^2 \tag{139}$$

This function is positive definite. Additionally, note that:

$$\|\mathbf{e}_x\| \leq \sqrt{2V_{x_2}} \tag{140}$$

$$\|\dot{\mathbf{e}}_x\| \leq \sqrt{\frac{2}{m_Q}V_{x_2}} \tag{141}$$

Taking the derivative of the proposed function:

$$\dot{V}_{x_2} = \mathbf{e}_x \cdot \dot{\mathbf{e}}_x + m_Q\dot{\mathbf{e}}_x \cdot \ddot{\mathbf{e}}_x \tag{142}$$

Recall that from the equations of motion, the error dynamics are:

$$\begin{aligned}m_Q\ddot{\mathbf{e}}_x &= m_Q\ddot{\mathbf{x}} - m_Q\ddot{\mathbf{x}}^d \\ &= -m_Q g\mathbf{e}_3 + f\mathbf{b}_3 - m_Q\ddot{\mathbf{x}}^d\end{aligned}$$

Substituting this into the derivative of the Lyapunov function gives:

$$\begin{aligned}\dot{V}_{x_2} &= \mathbf{e}_x \cdot \dot{\mathbf{e}}_x + \dot{\mathbf{e}}_x \cdot (m_Q g\mathbf{e}_3 + f\mathbf{b}_3 - m_Q\ddot{\mathbf{x}}^d) \\ &\leq \|\mathbf{e}_x\|\|\dot{\mathbf{e}}_x\| + \|\dot{\mathbf{e}}_x\|\|- m_Q g\mathbf{e}_3 + f\mathbf{b}_3 - m_Q\ddot{\mathbf{x}}^d\| \\ &\leq \|\mathbf{e}_x\|\|\dot{\mathbf{e}}_x\| + \|\dot{\mathbf{e}}_x\|Y + \|\dot{\mathbf{e}}_x\||f| \\ &= \|\mathbf{e}_x\|\|\dot{\mathbf{e}}_x\| + \|\dot{\mathbf{e}}_x\|Y + \\ &\quad \|\dot{\mathbf{e}}_x\|\| - K_p\mathbf{e}_x - K_d\dot{\mathbf{e}}_x + m_Q g\mathbf{e}_3 + m_Q\ddot{\mathbf{x}}^d\| \\ &\leq (1+K_p)\|\mathbf{e}_x\|\|\dot{\mathbf{e}}_x\| + 2\|\dot{\mathbf{e}}_x\|Y + K_d\|\dot{\mathbf{e}}_x\|^2\end{aligned}$$

Using Eqs. 140 and 141:

$$\begin{aligned}\dot{V}_{x_2} &\leq 2(1+K_p)\sqrt{\frac{1}{m_Q}}V_{x_2} + 2Y\sqrt{\frac{2}{m_Q}V_{x_2}} + 2\frac{K_d}{m_Q}V_{x_2} \\ &= \beta_1 V_{x_2} + \beta_2\sqrt{V_{x_2}},\end{aligned}$$

where:

$$\beta_1 = 2(1+K_p)\sqrt{\frac{1}{m_Q}} + 2K_d$$

$$\beta_2 = 2Y\sqrt{\frac{2}{m_Q}}$$

When $V_{x_2} \geq 1$, $\sqrt{V_{x_2}} \leq V_{x_2}$. Assume there exists a time interval $[t_a, t_b] \subset [0, t^*]$ where $V_{x_2} \geq 1$. In this interval:

$$\dot{V} \leq (\beta_1 + \beta_2)V_{x_2} \tag{143}$$

Recall the Comparison Lemma: give the differential equation $\dot{u} = f(t,u)$, where $f$ is continuous in $t$ and locally Lipschitz in $u$ in a domain $\mathcal{D}$ and time $[t_0, t_1)$, with initial condition $u(t_0) = u_0$. If a second continuous function $v(t)$ satisfies $D^+v(t) \leq f(t,v)$, $v(t_0) \leq u_0$, on the domain $\mathcal{D}$ and time $[t_0, t_1)$, then $v(t) \leq u(t)$ for all $[t_0, t_1)$ [10].

Applying this to Eq. 143 gives:

$$V_{x_2}(t) \leq V_{x_2}(t_a)e^{(\beta_1+\beta_2)(t-t_a)}$$

For any time interval $[t_a, t_b] \subset [0, t^*]$ when $V_{x_2} \geq 1$, $V_{x_2}$ is bounded, and therefore, the error states are bounded. Thus, for the remaining time intervals when $V_{x_2} < 1$, $V_{x_2}$ is bounded as well, since as soon as the function increases to 1, it will become bounded. Thus, the error states are bounded for all of $[0, t^*]$ and the origin of the error states is exponentially attractive.

## REFERENCES


[1] GmbH Ascending Technologies. http://www.asctec.de.

[2] Federico Augugliaro, Angela P. Schoellig, and Raffaello DAndrea. Dance of the flying machines: Methods for designing and executing an aerial dance choreography. *IEEE Robotics Automation Magazine*, 20(4):96–104, Dec 2013.

[3] Markus Bernard and Konstantin Kondak. Generic slung load transportation system using small size helicopters. In *IEEE International Conference on Robotics and Automation (ICRA)*, 2009.

[4] Francesco Bullo and Andrew D. Lewis. *Geometric Control of Mechanical Systems*, volume 49 of *Texts in Applied Mathematics*. Springer Verlag, New York-Heidelberg-Berlin, 2004. ISBN 0-387-22195-6.

[5] Aleksandra Faust, Ivana Palunko, Patricio Cruz, Rafael Fierro, and Lydia Tapia. Learning swing-free trajectories for UAVs with a suspended load. In *IEEE International Conference on Robotics and Automation (ICRA)*, 2013.

[6] Aleksandra Faust, Ivana Palunko, Patricio Cruz, Rafael Fierro, and Lydia Tapia. Aerial suspended cargo delivery through reinforcement learning. In *Technical Report TR13-00, Department of Computer Science, University of New Mexico*, 2013.

[7] Markus Hehn and Raffaello DAndrea. Real-time trajectory generation for interception maneuvers with quadrocopters. In *IEEE/RSJ International Conference on Intelligent Robots and Systems (IROS)*, pages 4979–4984, Oct 2012.

[8] Markus Hehn, Robin Ritz, and Raffaello D'Andrea. Performance benchmarking of quadrotor systems using time-optimal control. *Autonomous Robots*, 2012.

[9] Sertac Karaman and Emilio Frazzoli. Sampling-based algorithms for optimal motion planning. *The International Journal of Robotics Research (IJRR)*, 2011.

[10] Hassan K. Khalil. *Nonlinear Systems*. Prentice Hall, 3 edition, December 2001. ISBN 0130673897.

[11] Steven M. Lavalle, James J. Kuffner, and Jr. Rapidly-exploring random trees: Progress and prospects. In *Algorithmic and Computational Robotics: New Directions*, pages 293–308, 2000.

[12] Taeyoung Lee. *Computational geometric mechanics and control of rigid bodies*. PhD thesis, University of Michigan, 2008.

[13] Taeyoung Lee, N. Harris McClamroch, and Melvin Leok. A lie group variational integrator for the attitude dynamics of a rigid body with applications to the 3d pendulum. In *IEEE Conference on Control Applications (CCA)*, pages 962–967, Aug 2005.

[14] Taeyoung Lee, Melvin Leok, and N. Harris McClamroch. Lagrangian mechanics and variational integrators on two spheres. In *International Journal for Numerical Methods in Engineering*, 2008.

[15] Taeyoung Lee, Melvin Leok, and N. Harris McClamroch. Control of complex maneuvers for a quadrotor UAV using geometric methods on SE(3). In *Asian Journal of Control*, 2011.

[16] Taeyoung Lee, Melvin Leok, and N. Harris McClamroch. Stable manifolds of saddle points for pendulum dynamics on $s^2$ and $so(3)$. In *IEEE Conference on Decision and Control*, page 39153921, Dec 2011.

[17] Taeyoung Lee, Koushil Sreenath, and Vijay Kumar. Geometric control of cooperating multiple quadrotor UAVs with a suspended payload. In *IEEE Conference on Decision and Control (CDC)*, 2013.

[18] Quentin Lindsey, Daniel Mellinger, and Vijay Kumar. Construction of cubic structures with quadrotor teams. In *Proceedings of Robotics: Science and Systems (ROSS)*, Los Angeles, CA, USA, June 2011.

[19] Daniel Mellinger and Vijay Kumar. Minimum snap trajectory generation and control for quadrotors. In *IEEE International Conference on Robotics and Automation (ICRA)*, 2011.

[20] Daniel Mellinger, Nathan Michael, and Vijay Kumar. Trajectory generation and control for precise aggressive maneuvers with quadrotors. In *Int. Symposium on Experimental Robotics (ISER)*, volume 79 of *Springer Tracts in Advanced Robotics*, pages 361–373. Springer, 2010.

[21] Daniel Mellinger, Alex Kushleyev, and Vijay Kumar. Mixed-integer quadratic program trajectory generation for heterogeneous quadrotor teams. In *IEEE International Conference on Robotics and Automation (ICRA)*, pages 477–483, May 2012.

[22] Nathan Michael, Daniel Mellinger, Quentin Lindsey, and Vijay Kumar. The grasp multiple micro-UAV testbed. *IEEE Robotics Automation Magazine*, 17(3):56–65, Sept 2010.

[23] Richard M. Murray, Muruhan Rathinam, and Willem Sluis. Differential flatness of mechanical control systems: A catalog of prototype systems. In *Proceedings of the 1995 ASME International Congress and Exposition*, 1995.

[24] James Potter, William Singhose, and Mark Costello. Reducing swing of model helicopter sling load using input shaping. In *IEEE International Conference on Control and Automation (ICCA)*, pages 348–353, Dec 2011.

[25] Charles Richter, Adam Bry, and Nicholas Roy. Polynomial trajectory planning for quadrotor flight. In *IEEE International Conference on Robotics and Automation (ICRA)*, 2013.

[26] Robin Ritz and Raffaello D'Andrea. Carrying a flexible payload with multiple flying vehicles. In *IEEE/RSJ International Conference on Intelligent Robots and Systems (IROS)*, pages 3465–3471, 2013.

[27] Shaojie Shen, Nathan Michael, and V. Kumar. Autonomous indoor 3d exploration with a micro-aerial vehicle. In *IEEE International Conference on Robotics and Automation (ICRA)*, pages 9–15, May 2012.

[28] Slobodan N. Simic, Karl Henrik Johansson, John Lygeros, and Shankar Sastry. Towards a geometric theory of hybrid systems. In *Hybrid Systems: Computation and Control*, 2000.

[29] Koushil Sreenath, Taeyoung Lee, and Vijay Kumar. Geometric control and differential flatness of a quadrotor UAV with a cable-suspended load. In *IEEE Conference on Decision and Control (CDC)*, 2013.

[30] Koushil Sreenath, Nathan Michael, and Vijay Kumar. Trajectory generation and control of a quadrotor with a cable-suspended load – a differentially-flat hybrid system. In *IEEE International Conference on Robotics and Automation (ICRA)*, 2013.

[31] Russ Tedrake. LQR-trees: Feedback motion planning on sparse randomized trees. In *Proceedings of Robotics: Science and Systems*, Seattle, USA, June 2009.

[32] Justin Thomas, Joe Polin, Koushil Sreenath, and Vijay Kumar. Avian-inspired grasping for quadrotor micro UAVs. In *ASME International Design Engineering Technical Conference (IDETC)*, 2013.

[33] Matthew Turpin, Nathan Michael, and Vijay Kumar. Capt: Concurrent assignment and planning of trajectories for multiple robots. *International Journal of Robotics Research*, 2012.

[34] Inc. Vicon Motion Systems. http://www.vicon.com.

[35] Youtube. Christmas trees 2010- putting trees in trucks. http://www.youtube.com/watch?v=SPO9pVwoxVg.